TÉCNICO LISBOA

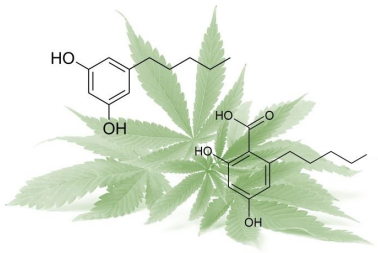

Studies on the uptake of olivetol and olivetolic acid by *Saccharomyces cerevisiae*

Juliana Andreia Falcão Estrela

Thesis to obtain the Master of Science Degree in

Biological Engineering

Supervisor(s): Prof. Dr. Oliver Kayser
Prof. Gabriel António Amaro Monteiro

Examination Committee

Chairperson: Prof. Arsénio do Carmo Sales Mendes Fialho
Supervisor: Prof. Gabriel António Amaro Monteiro
Member of the Committee: Prof. Pedro Carlos de Barros Fernandes

November 2016

Acknowledgments

I would like to address my most sincere gratitude to Professor Dr. Oliver Kayser for allowing me to write my thesis in the Technical Biochemistry department at TU Dortmund. It was a very interesting and stimulant project that allowed me to grow both personally and academically.

I would also like to thank to my supervisor at IST, Professor Gabriel Monteiro, for accepting to be my supervisor and for contributing to the improvement of my thesis.

I am very grateful for the guidance and support given by PhD student Sara-Friederike Degenhardt, as well as for her feedback on my thesis. Her orientation was very helpful for developing my practical work, as well as for the writing of my thesis.

I am very thankful to all the TB group. Everyone was always very supporting and helpful during my stay and it was really a pleasure to work with them.

I couldn't have done it without the support of my family and friends that were always ready to help me, despite the distance. Also, a big thanks to Pedro for his patience and love, especially in the most stressful moments.

Lastly, I would like to thank the National erasmus agency, for the scholarship provided during my stay abroad.

Resumo

A marijuana medicinal tem sido cada vez mais reconhecida ao longo dos últimos anos pelas propriedades terapêuticas associadas aos canabinóides, como por exemplo o tetrahidrocanabinol (THC), que apresentam eficácia no tratamento de certas condições médicas, bem como contra efeitos secundários provocados pelos tratamentos de certas doenças. No entanto, esta planta continua a ser ilegal na maior parte dos países. Eventualmente, esta situação leva à venda ilegal e não taxada de marijuana para auto-medicação ou à migração de pessoas de forma a poderem aceder a esta droga.

O principal objectivo deste projecto é fornecer ácido olivetólico, um dos percursores da biossíntese de canabinóides, a uma cultura de *Saccharomyces cerevisiae* para posterior produção heteróloga de ácido tetrahidrocanabinólico (THCA) neste hospedeiro.

Neste estudo em particular, foi verificado que o DMSO, o principal solvente para o olivetol e para o ácido olivetólico, é tóxico para esta estirpe específica de *S. cerevisiae* em concentrações superiores a 3 % (v/v). Verificou-se também que o olivetol tem um efeito inibitório no crescimento de *S. cerevisiae*, visto que se pode verificar um aumento no tempo de adaptação e no tempo de duplicação e uma diminuição na taxa específica de crescimento com o aumento da concentração de olivetol. Além disto, quando as culturas celulares desta levedura são expostas a olivetol/ácido olivetólico, verifica-se que há um aumento na concentração destes compostos na fração celular ao longo do tempo, que pode ser uma captação ou não, mas que ocorre simultaneamente a uma diminuição da concentração destes compostos no meio de cultura.

Palavras-chave: Ácido olivetólico; olivetol; captação; canabinóides; *Saccharomyces cerevisiae*.

Abstract

Medical marijuana has had an increasing recognition over the last few years for the medical properties presented by its cannabinoids, such as THC, effective either towards side effects caused by the treatment for several diseases, or as a therapeutic agent towards certain conditions. Nevertheless, it remains illegal in the majority of countries. This eventually leads to non-taxed illicit sale of marijuana for self-medication or to the migration of people for an opportunity to access this drug.

The main purpose of this study is to feed olivetolic acid, one of the percursors for cannabinoid biosynthesis, to *Saccharomyces cerevisiae* for further heterologous production of tetrahydrocannabinolic acid (THCA) by this microbial host.

In this specific project, it was shown that DMSO, the main solvent for olivetol and olivetolic acid, is toxic to this specific strain of *S. cerevisiae* for concentrations higher than 3 % (v/v) and that olivetol has an inhibitory effect on the growth of *S. cerevisiae*, which can be verified by the increasing lag time and doubling time, as well as by the decrease in the specific growth rate with an increasing concentration of olivetol. Furthermore, when cell cultures of this yeast are exposed to olivetol/olivetolic acid, there is an increasing concentration of these compounds in the cell fraction over time, that can either be an uptake or not, combined with a decreasing concentration of this compound in the cell culture medium.

Keywords: Olivetolic acid; olivetol; uptake; cannabinoids; *Saccharomyces cerevisiae*.

Contents

List of Tables

List of Figures

Nomenclature

Δ^9-THC, THC Tetrahydrocannabinol.

Δ^9-THCA, THCA Tetrahydrocannabinolic acid.

A Absorbance.

AAC Acyl-activating enzyme.

AIDS Acquired immune deficiency syndrome.

bp Base pairs.

CBC Cannabichromene.

CBCA Cannabichromenic acid.

CBCAS Cannabichromenic acid synthase.

CBD Cannabidiol.

CBDA Cannabidiolic acid.

CBDAS Cannabidiolic acid synthase.

CBG Cannabigerol.

CBGA Cannabigerolic acid.

CBGAS Cannabigerolic acid synthase.

CBGVA Cannabigerovarinic acid.

CBNRA Cannabinerolic acid.

dH_2O Distilled water.

DABB Dimeric $\alpha + \beta$ barrel.

DMAPP Dimethylallyl diphosphate.

DMSO Dimethylsulfoxide.

DNA Deoxyribonucleic acid.

DTT Dithiothreitol.

EDTA Ethylenediaminetetraacetic acid.

EST Expressed sequence tag.

GOT Geranyldiphosphate:olivetolate geranyltransferase.

GPP Geranyl diphosphate.

GPPS Geranyl diphosphate synthase.

HIV Human immunodeficiency virus.

HPLC High performance liquid chromatography.

HTAL Hexanoyl triacetic acid lactone.

I Intensity of outgoing light.

I_0 Intensity of incoming light.

IPP Isopentenyl diphosphate.

NPP Neryl pyrophosphate.

OA Olivetolic acid.

OAC Olivetolic acid cyclase.

OD Optical density.

PDAL Pentyl diacetic acid lactone.

PEG Poliethylene glycol.

PMSF Phenylmethylsulfonyl fluoride.

rpm Rotations per minute.

THCAS Tetrahydrocannabinolic acid synthase.

TKS Tetraketide synthase.

UV Ultraviolet.

yEGFP Yeast-enhanced green fluorescent protein.

Chapter 1

Introduction

1.1 Motivation

Cannabis sativa, also known as marijuana, weed, hemp or just cannabis, was considered the most widely used illicit drug in the world, in a study conducted in 2015 [1].

Even though the public opinion on medical marijuana has always shown a tendency towards its legalization, with an increase in this general opinion over the last few years, the use of this plant remains forbidden in many countries.

Even though chemical synthesis of tetrahydrocannabinolic acid (THCA) and cannabidiolic acid (CBDA), the main compounds found in cannabis with therapeutic potential, seems the clear solution to overcome these legal barriers, it has proven not to be very efficient.

Another possible pathway for obtaining THCA and CBDA would be the extraction of these compounds from the cannabis plant. Even though this approach is followed nowadays, the cultivation of this plant is forbidden in the majority of countries and it is also not very efficient.

One of the solutions for the production of these compounds may be the the heterologous production of cannabinoids in microbial hosts.

1.2 Topic Overview

The effectiveness of cannabinoids in treating several medical conditions has been well documented, and it shows positive results, either towards some conditions with an ineffective treatment, or towards the side effects caused by a number of therapies.

C. sativa produces a group of terpenophenolics referred to as cannabinoids, which include its major psychoactive component, Δ^9-tetrahydrocannabinol (Δ^9-THC), that presents medicinal properties towards at least 10 different pathologies, such as nausea and vomiting associated with cancer chemotherapy, multiple sclerosis, Tourette's syndrome, epilepsy, glaucoma and Parkinson's disease [2].

Along with Δ^9-THC, both cannabidiol (CBD) and cannabichromene (CBC) show therapeutic properties. The first one shows high anti-oxidant and anti-inflammatory properties, which can provide neuro-

protection against chronic and acute neurodegeneration. These properties can be effective against the toxicity caused by 6-hydroxydopamin, which can be relevant for the treatment of Parkinson disease. The second one shows anti-inflammatory, antifungal and antibacterial properties [3].

1.3 Objectives

Considering that the cannabis plant is still illegal for medical use in most countries, the main purpose of the studies performed at the TB department in TU Dortmund is the genetic manipulation of microbial hosts, in order to produce THCA heterologously.

Currently, several approaches are being tested in order to clone the genes present in *Cannabis sativa* that express the necessary enzymes for synthesizing THCA, in microbial hosts such as *Pichia pastoris* or *Saccharomyces cerevisiae*. The final objective of the project is to feed the percursors of cannabigerolic acid (CBGA), olivetolic acid (OA) and geranyl diphosphate (GPP), to the desired host, in order to synthesize CBGA and further obtain Δ^9-THCA and CBDA through enzymatic reactions.

One approach that has been already tested was the production of olivetolic acid inside the microbial host. Unfortunately, although this approach showed positive results and the production of olivetolic acid was optimized, the amounts produced were not significant for the production of cannabigerolic acid.

The main scope of this particular project was to evaluate the behaviour of a specific strain of *Saccharomyces cerevisiae* when olivetolic acid was fed in different concentrations, as well as evaluating whether it would be capable of uptaking it. Finally, upon successful uptake, the final site of accumulation of olivetolic acid would be evaluated.

1.4 Thesis Outline

In this work, the biosynthesis of cannabinoids is briefly explained, along with a description of the social context of cannabis use, in chapter 2. Further on, the materials used and the methods followed during laboratorial practice are described on chapter 3. Chapter 4 encompasses the main results obtained and the discussion of these results, along with some conclusions that could be taken, as well as with some details that should be further studied. Lastly, chapter 5 shows a compilation of the main conclusions taken and suggestions for further studies on the subject of this project.

Chapter 2

Background

2.1 The social context of cannabis use

Cannabis sativa, also known as marijuana, hemp, weed or just cannabis (see figure 2.1), is the most used illicit drug worldwide, according to the World Drug Report released in 2015 [1], with an estimated number of users between 128 and 232 million people.

Figure 2.1: Painting of *Cannabis sativa* from Köhler (1887). **A** Flowering male branch. **B** Fruiting female branch. **C** Cluster of male flowers. **D** Fruit (achene) surrounded by perigonal bract. **E** View of wide (flat) side of achene. **F** View of narrow side of achene. **G** Pistil, showing ovary and two stigmatic branches. **H** Pistil surrounded by young perigonal bract.

Along with hops, it belongs to the *Cannabaceae* family and its origin can be traced to Central Asia. The beginning of its use is unknown, since it is prior to the invention of writing [2]. *Cannabis sativa* is a dioecious plant that shows a particular group of secondary metabolites, the cannabinoids, that, despite being present in other plants, such as *Echinacea purpurea*, *Echinacea angustifolia* or *Acmella oleracea*, are very characteristic of *Cannabis sativa* [4].

This plant can be classified into two types: the drug-type and the fiber-type, which correspond to two different strains, which are associated with its psychoactive effect and with its use as a textile fiber, respectively. Chemically, both types show differences, especially in their cannabinoid content: the drug-type shows high amount of THCA and almost no CBDA and the fiber-type shows high amounts of CBDA and almost no THCA. Regarding cannabichromenic acid (CBCA), both types show approximately the same amount [3]. Nowadays, although it lost some of its value and it is only used in niche markets, hemp fibers are used for pulp products and composites, such as fiberboard, insulation, carpets and a wide range of plastics, among others. For more than 3000 years, cannabis seeds have also been used for the production of hemp oil, which has gained recognition nowadays for its health benefits. It is also used in nutritional cosmetics and as an industrial fluid [5].

However, one of the most relevant characteristics of this plant is its therapeutic effect. Some examples include its use as an appetite stimulant for the treatment of anorexia, cancer and HIV/AIDS [6] [7] [8] or its antiemetic use by cancer chemotherapy patients [9] [10] [11]. It also provides chronic neuropathic pain relief for cancer, HIV/AIDS and other types of chronic pain, such as fibromyalgia and rheumatoid arthritis [12] [13] [14] and multiple sclerosis [15] [16] [17]. Furthermore, there have been emerging reports showing positive results for the use of cannabis as a treatment for a number of cancers [18] [19] [20] [21], epilepsy [22] [23], Alzheimer's disease [24] [25], Huntington's disease [26] [27], diabetes [28] [29] and Tourette's syndrome [30] [31].

The two main cannabinoids that have been studied for their therapeutic potential are THC and CBD, which are naturally present in the cannabis plant in its acidic form, THCA and CBDA respectively. THC, the psychoactive agent of cannabis, has anti-inflammatory, analgesic, appetite-stimulant and antiemetic properties [32]. On the other hand, CBD controls the euphoric effects of THC and has antipsychotic, neuroprotective, anticancer and antidiabetic as well as other positive effects, such as the potential to reduce tobacco addiction [33] [34] [35] [36] [37]. Although present studies have not focused so much on it, cannabigerol (CBG) also shows therapeutic effects against glaucoma [38], inflammatory bowel disease [39] and prostate carcinoma [40]. CBC has analgesic effects [41], the potential to stimulate the growth of brain cells [42] and the ability to normalize gastrointestinal hypermotility [43].

Considering that cannabis also has a considerable amount of CBC, the combined effect of both CBC and Δ^9-THC was studied. Their combined action failed to prevent induced seizures, but showed an improved analgesic effect when combined with and even when compared to morphine, for a long period of time [44].

However, Δ^9-THC accumulates in small levels in the fresh leaves of *C. sativa*, and it is only formed during storage, smoking or baking due to the decarboxylation of its acidic correspondent cannabinoid, tetrahydrocannabinolic acid [45].

2.2 Cannabinoids and their biosynthesis

More than 100 cannabinoids have been identified until today, and the most relevant, besides Δ^9-THC, include CBG, CBD, CBC and cannabinol (CBN), which have little to no psychoactive effect [2] [5] [46]. These cannabinoids are also referred to as phytocannabinoids, in order to distinguish them from synthetic cannabinoids, and from a group of endogenous cannabinoid receptors in mammal tissues that were identified in the 90's, the endocannabinoids [47].

The endocannabinoid system shows high-affinity, saturable, stereospecific binding sites for cannabinoids and comprises two types of receptors: the CB_1 receptors, which are the receptors associated with the nervous system and are the most abundant in the mammalian brain, and the CB_2 receptors, that are associated with the immune system and are expressed primarily in cells of the immune and hematopoietic systems. Δ^9-THC is the most potent phytocannabinoid activator of the CB_1 receptor and it is only synthesized naturally in the cannabis plant, mostly in its acidic form [48].

Nowadays, there are already pharmaceutical drugs available that contain either cannabinoids extracted from *Cannabis sativa*, such as Sativex ® oral spray, or that contain synthetic versions of chemicals naturally found in marijuana, such as Marinol ®, which is synthetic Δ^9-THC, also known as dronabinol.

Although chemical synthesis of cannabinoids is a possible way of having access to these therapeutic drugs, it has proven not to be very efficient. The main problem faced during chemical synthesis is the fact that the Δ^8-THC isomer is more stable than Δ^9-THC, being the last one the desired chemical compound (see figure 2.2).

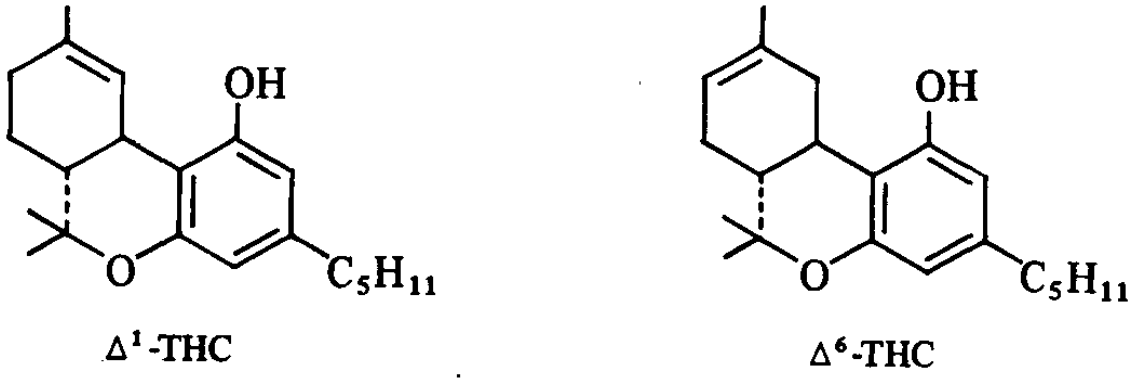

Figure 2.2: Chemical structure of Δ^1-THC and Δ^6-THC also known as Δ^9-THC and Δ^8-THC respectively under the monoterpenoid and dibenzopyran numbering systems respectively [49].

Cannabinoid acids, such as Δ^9-THCA, CBDA and CBCA are naturally produced in the cannabis plant through a series of enzymatic reactions and are then converted to their neutral forms (Δ^9-THC, CBD and CBC respectively) through a non-enzymatic decarboxylation reaction. The neutral form of Δ^9-THCA is the psychoactive agent of cannabis, and the reason why the consumption of marijuana usually involves heating of the material (smoking or baking), is to decarboxylate this acid [3]. Even though enzymatic reactions play an important part on the biosynthesis of cannabinoids, the majority of these compounds are formed through transformation or degradation of both acidic and neutral cannabinoids by the effects

of light (UV irradiation) and auto-oxidation [50] [51].

Being a dioecious plant, *Cannabis sativa* can occur in both female and male forms, but only the female plant contains cannabinoids. These cannabinoids accumulate mainly in the secretory cavity of the glandular trichomes of the female plants [5].

The two main percursors for cannabinoid biosynthesis are geranyl diphosphate and olivetolic acid, which are converted to cannabigerolic acid (CBGA) in a reaction catalysed by cannabigerolic acid synthase (CBGAS).

2.2.1 Biosynthesis of geranyl diphosphate

Geranyl diphosphate, or GPP, is the percursor responsible for providing the characteristic terpenoid moiety of cannabinoids (represented in red in figure 2.3). In a study conducted by Fellermeier and coworkers [52], it has been shown, through labelling pattern studies, that GPP derives predominantly (98 %) from the deoxyxylulose pathway (MEP/DOXP), which takes place in the plastid compartments of the *Cannabis sativa* trichomes. There is also a minor contribution of the mevalonate pathway (MVA) for GPP biosynthesis. This is possible because there is no absolute compartmental separation between both pathways and there is a cross-talk of these two terpenoid biosynthetic pathways [53].

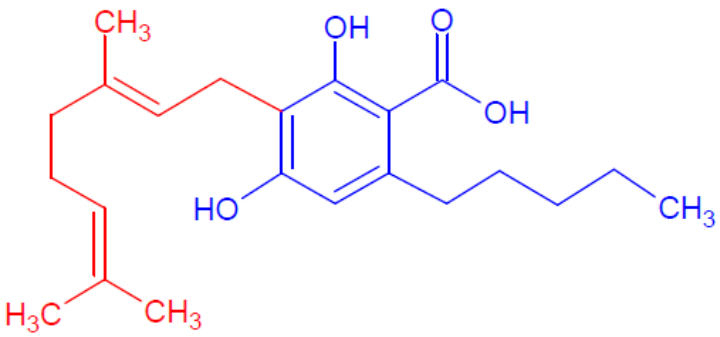

Figure 2.3: Chemical structure of CBGA with the terpenoid moiety represented in red and the alkylresorcinol moiety represented in blue.

The *cis*-isopentenyl diphosphate (*cis*-IPP), or just IPP, derived from these pathways is then converted to dimethylallyl diphosphate, or DMAPP, the *trans* isomer of IPP, in a reaction catalysed by IPP isomerase. Geranyl diphosphate synthase (GPPS), an enzyme that was cloned, expressed and characterized by Burke et. al [54] in 1999, will then catalyse the condensation between two molecules of DMAPP to synthesize GPP. This enzyme can also catalyse the condensation between DMAPP and IPP, originating neryl diphosphate (NPP).

A scheme representing the synthesis of GPP and NPP is shown on figure 2.4.

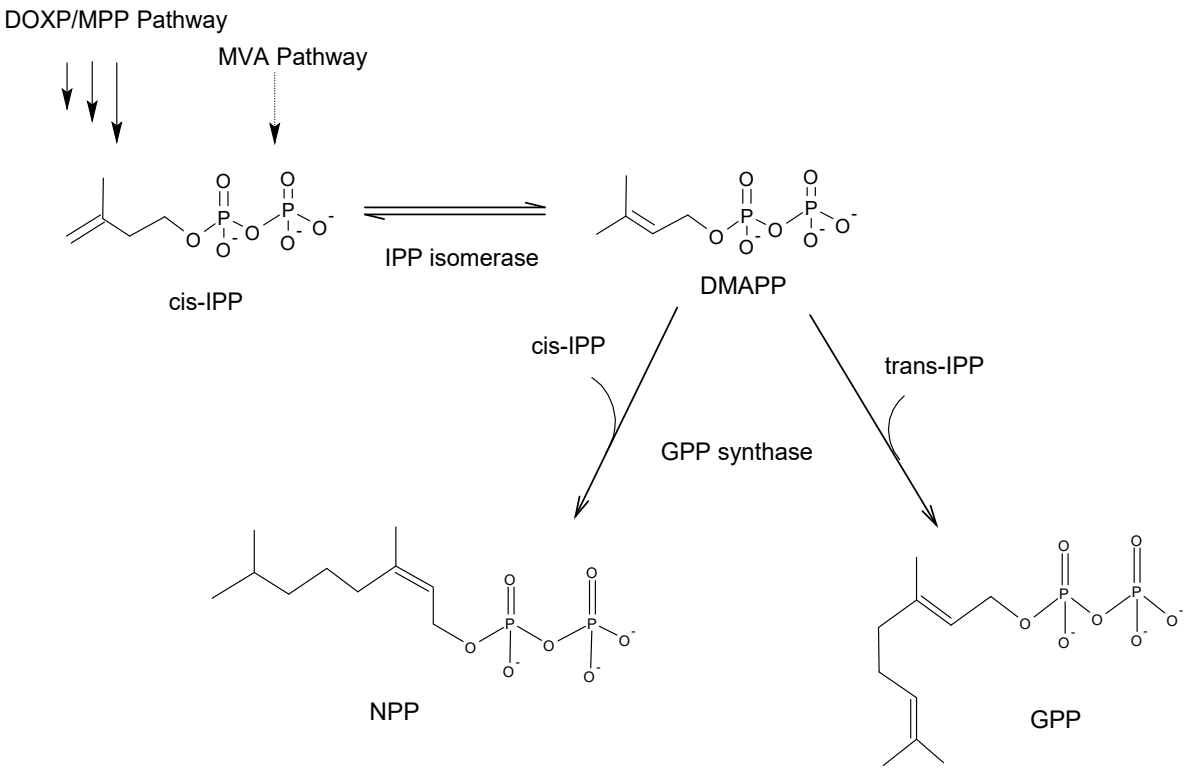

Figure 2.4: Scheme representing the synthesis of GPP and NPP.

2.2.2 Biosynthesis of olivetolic acid

Olivetolic acid is the percursor in the biosynthesis of CBGA that will provide the characteristic alkyl-resorcinol moiety of this cannabinoid (see blue moiety of molecule represented in figure 2.3).

The biosynthesis of olivetolic acid starts with a molecule of hexanoate. The origin of the hexanoate for the synthesis of this compound is still unknown, but in a study conducted by Fellermeier in 2001 [52] it was shown that the hexanoate is synthesized from acetyl-CoA and five molecules of malonyl-CoA, known percursors of fatty acid biosynthesis.

According to Marks et. al [55], there are two possible ways for obtaining this hexanoate molecule. The first theory defends that the early termination of the fatty acid biosynthesis yields hexanoyl-ACP and, afterwards, there are two possibilities. Either a thiesterase cleaves this molecule, yielding n-hexanol that is converted to n-hexanoyl-CoA by an acyl-CoA synthase, or an ACP-CoA transacylase transfers the hexanoyl moiety of this compound to CoA. According to the second possible theory, there is the breakdown of linoleic acid via the lipoxygenase (LOX) pathway, which is converted to hexanoyl-CoA by an acyl-CoA synthase.

In the same study conducted by Marks et. al in 2009 [55], the RNA from the secretory glands of a Δ^9-tetrahydrocannabinolic acid (THCA)-producing strain of *Cannabis sativa* was isolated and a cDNA library of expressed sequence tags (ESTs) was generated. These sequenced ESTs were further analysed and genes encoding the enzymes necessary for synthesis of linoleic acid from acetyl-CoA were identified. Furthermore, genes encoding enzymes necessary for the production of hexanol from linoleic acid via the

LOX pathway were also identified. In a study conducted in 2012 by Stout et. al [56], it was shown that the formation of hexanoyl-CoA from hexanoate and a CoA unit is catalysed by hexanoyl-CoA synthetase, an acyl-activating enzyme (AAC).

Even though these results support the second theory, further studies are necessary to confirm the origin of the hexanoate in the biosynthesis of olivetolic acid.

From this point on, several studies have been published in an effort to identify the enzymes responsible for catalysing the condensation of hexanoyl-CoA with three molecules of malonyl-CoA to yield olivetolic acid. A polyketide synthase (PKS), which was named olivetol synthase was identified by Taura et. al in 2009 [57], but when expressed in *E. coli* and fed malonyl-CoA and hexanoyl-CoA, it could only produce pentyl diacetic acid lactone (PDAL) and hexanoyl triacetic acid lactone (HTAL), as well as olivetol, but not olivetolic acid. In a study conducted in 2012 by Gagne et. al [58], olivetol synthase was renamed tetraketide synthase (TKS) and the polyketide cyclase necessary for the final cyclization reaction was identified. This enzyme, which was named olivetolic acid cyclase (OAC), is mainly expressed in the trichomes of the cannabis plant, but also in the flowers in lower amounts. It is a dimeric $\alpha + \beta$ barrel (DABB) protein and the specific reaction catalised by it involves an aldol cyclization C2 $\rightarrow$ C7, cleavage of the thioesther bond and an aromatization.

The combined action of this two enzymes leads to the formation of olivetolic acid, as well as HTAL, PDAL and olivetol as by-products. Note that these enzymes have a combined action, but do not interact with each other. Alongside these products, divarinic acid is also formed, being the mechanism leading to its formation still unknown. Divarinic acid is identical to olivetolic acid, except for a hydrocarbon chain coming off the phenolic ring, which in the latter is slightly longer (see figure 2.5). A scheme representing the synthesis of olivetolic acid and by-products is shown on figure 2.6.

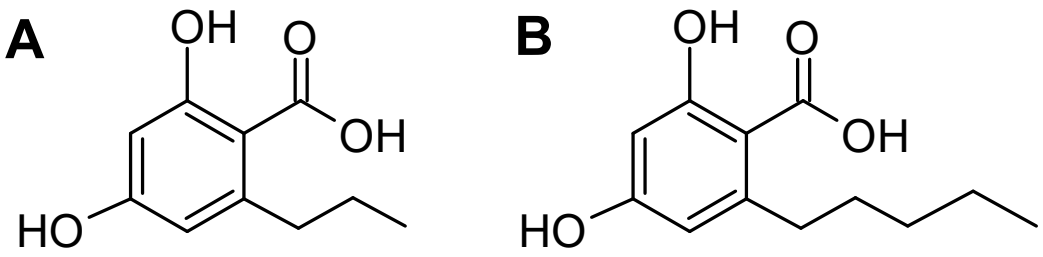

Figure 2.5: Chemical structure of divarinic acid (molecule A) and olivetolic acid (molecule B).

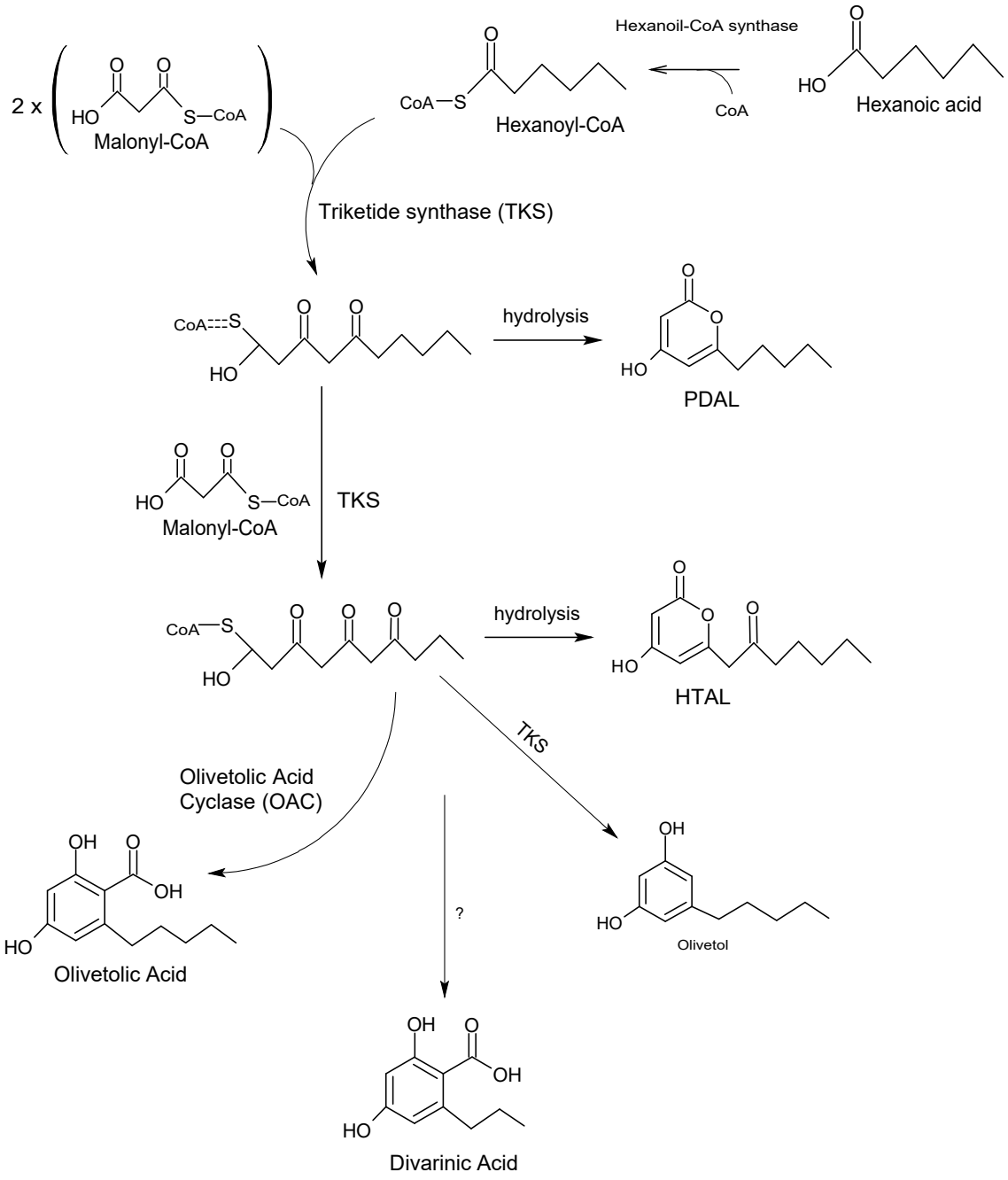

Figure 2.6: Scheme representing the synthesis of olivetolic acid and by-products.

2.2.3 Biosynthesis of cannabigerolic acid

The next step on the biosynthesis of cannabinoids is the synthesis of CBGA. This is a condensation reaction that is catalysed by an enzyme named cannabigerolic acid synthase (CBGAS), which is a prenyltransferase. In this reaction, CBGAS catalyses the C-prenylation of OA by GPP.

This enzyme was first detected in extracts of young leaves of *Cannabis sativa* by Fellermeier et. al in 1998 [46] and it was named geranylpyrophosphate:olivetolate geranyltransferase (GOT). In the same study it was shown that this enzyme only accepts olivetolic acid as a prenyl acceptor, but accepts GPP and NPP to a lesser degree, as a prenyl donor, in order to form CBGA and cis-CBGA (or cannabinerolic acid, CBNRA) respectively. Only later on, in 2009, did de Meijer and coworkers [59] report that CBGAS could use divarinic acid as a prenyl acceptor and its condensation with GPP yields cannabigerovarinic acid (CBGVA). Nevertheless, the neutral analogue of olivetolic acid, olivetol, cannot be used as a prenyl acceptor. When using GPP as a prenyl donor, CBGA and cannabinerolic acid (CBNRA or cis-CBGA) are synthesized in a 2:1 ratio. On the other hand, if both GPP and NPP are used as prenyl donors, this ratio changes to 1:1. If only NPP is fed to CBGAS in the presence of OA, only cis-CBGA is formed [46].

It was expected that CBGAS would be a membrane-bound enzyme, when comparing with other prenyltransferases. However, in the previously referred study, conducted by Fellermeier and Zenk in 1998 [46], this enzyme was not found in the particulate fraction, but in the soluble fraction of the crude extract. Nevertheless, all the aromatic prenyltransferases present in plants are membrane-bound, and the first hypothesis could not be excluded.

In a study published in 2012 conducted by Page and Boubakir [60], the sequence of CBGAS was published and it showed that this enzyme is expressed in the female flowers and in young leaves of *Cannabis sativa*. It also showed that this gene encodes a 395-amino acid polypeptide chain showing a membrane-bound type of prenyltransferases.

After the biosynthesis of CBGA, the majority of cannabinoids will be synthesized through enzymatic and non-enzymatic reactions.

2.2.4 Further biosynthesis of cannabinoids

After the synthesis of CBGA, the three main cannabinoid acids will be synthesized through the stereoselective oxidative cyclization of the monoterpene moiety of CBGA. These three cannabinoid acids are Δ^9-tetrahydrocannabinolic acid (Δ^9-THCA, or just THCA), cannabidiolic acid (CBDA) and cannabichromenic acid (CBCA) by the action of tetrahydrocannabinolic acid synthase (THCAS), cannabidiolic acid synthase (CBDAS) and cannabichromenic acid synthase (CBCAS) respectively. Each of these cannabinoids acids is then converted to its neutral form, Δ^9-tetrahydrocannabinol (Δ^9-THC, or just THC), cannabidiol (CBD) and cannabichromene (CBC) through non-enzymatic decarboxylation.

It is important to note that the reactions catalysed by the previously mentioned enzymes do not occur when using the neutral analogues of the substrate (CBG), leading to believe that the carboxyl group is essential for enzymatic activity [61] [62] [63].

In a study conducted by Sirikantaramas in 2005 [64], it was reported that THCAS is an enzyme

that is secreted in the secretory cells of the glandular trichome of cannabis and that there is a sorting pathway that leads it to the storage cavity of the trichomes, suggesting that this is not only the site for accumulation of cannabinoids, but also the site for THCA biosynthesis. Furthermore, in the same study, it was concluded that both THCA and CBGA induce cell death. Considering this and the fact that hydrogen peroxide is also produced during the synthesis of THCA, it was concluded that these two enzymes (THCAS and CBGAS) contribute to the self-defense of the cannabis plant by producing these cannabinoids along with H_2O_2. In order to avoid cellular damage on the cell, this synthesis occurs in the storage cavity.

Even though these tests were not performed on CBDA and CBCA, one could assume that they are likely to show these same properties and are also involved in the self-defense of the plant.

From this point on, the remaining cannabinoids are synthesized through non-enzymatic transformations. It is important to note that besides THCA, CBDA and CBCA, cannabinerolic acid (CBNA) and cannabigerovarinic acid (CBGVA) are also percursors for further synthesis of cannabinoids, even though in a much lower amount.

The complete synthesis of cannabinoids is shown in figure 2.7.

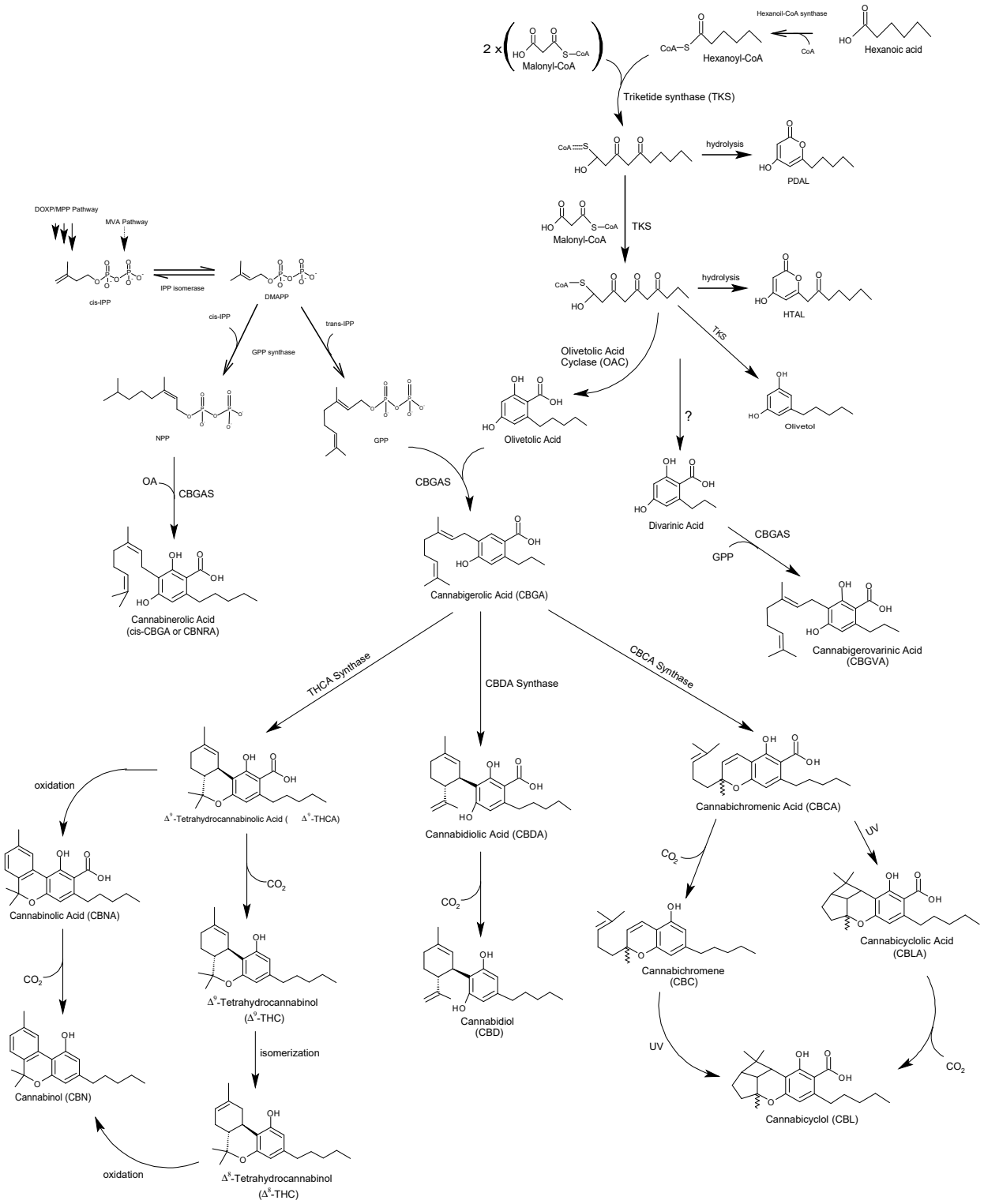

Figure 2.7: Schematic representation of the synthesis of the main cannabinoids.

2.3 Growth of *Saccharomyces cerevisiae*

Saccharomyces cerevisiae is an eukariotic microbe known by its role in food production. Nevertheless, considering that it is the most studied eukariote, it can be a very good microbial host for the production of heterologous products.

Reconstructing biosynthetic pathways in microbial hosts brings several advantages. One of them is the fact that it leads to a lower loss of pathway intermediates to competing pathways and can provide the possibility to change the biosynthetic pathway, in order to produce more powerful analogues. A microbial host also provides a rapid growth rate which leads to higher productivity and the availability of multiple genetic engineering tools to optimize the pathway [65].

2.3.1 The growth curve of *Saccharomyces cerevisiae*

The growth curve of *Saccharomyces cerevisiae* was first described by Richards in 1928 [66]. In figure 2.8 it is possible to see an example of such.

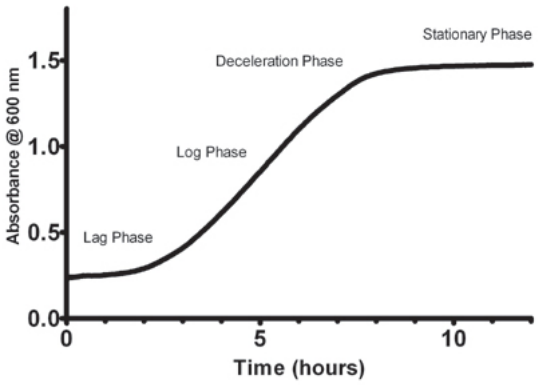

Figure 2.8: Growth curve of *Saccharomyces cerevisiae*. The optical density at a wavelength of 600 nm is represented over time. [67]

As it is possible to see in figure 2.8, a growth curve usually comprises five main stages: the lag phase, the exponential phase (log phase), the deceleration phase, the stationary phase and the death phase (not represented).

The lag phase is usually characterized by an adaptation from the cells to the new culture conditions, being desirable a small lag phase.

The exponential phase is the phase during which the concentration of cells rises exponentially with time.

The deceleration phase, as the name says, is the phase in which the cell growth starts being less steep, but there is still some growth. This is a transition phase between the exponential and the stationary phases.

The stationary phase is the phase in which the cell concentration is constant, even though the percentage of non-viable cells increases with time. This phase is usually associated with carbon source depletion and with the formation of toxic metabolites.

Lastly, in the death phase, there is a decrease in the number of viable cells, being this phase associated with cell lysis [68].

2.3.2 The Crabtree effect

The diauxic growth of yeast (see figure 2.9) was first described in 1954 [69]. Lemoigne, Aubert and Millet showed that when exposed to high concentrations of glucose, cell cultures of baker's yeast that were exposed to air would present two growth phases. The first one would show a fast growth associated with intensive aerobic fermentation, followed by stationary phase. The second growth phase, on the other hand, shows a slow growth rate which is associated with the oxidation of the accumulated ethanol that has been produced in the first growth phase.

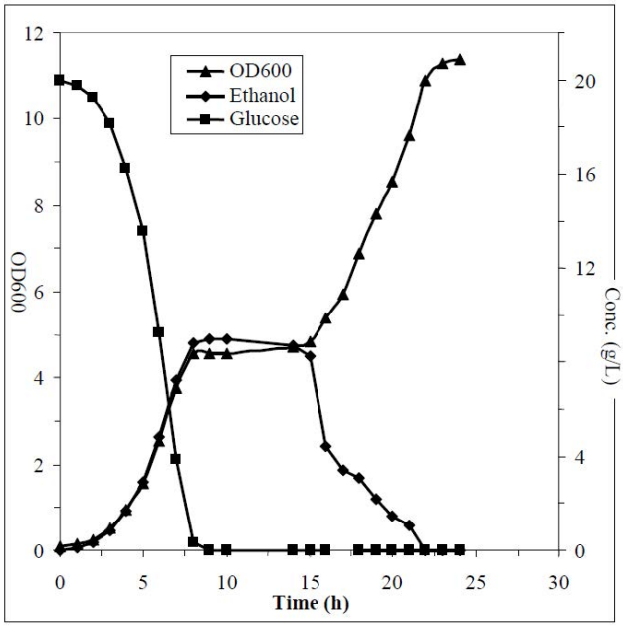

Figure 2.9: Diauxic growth curve of *Saccharomyces pastorianus*, representing consumption of glucose, production of ethanol and consumption of ethanol over time [70].

It was further reported by Slonimski in 1956 [71] that for concentrations of glucose higher than 6 mM, the yeast uses aerobic fermentation rather than respiration. This was described as the Crabtree effect in 1966 by De Deken [72]. In this study, it was reported that when cultures of *Saccharomyces cerevisiae* are exposed to high concentrations of glucose in aerobic conditions, there is a repression of the respiration pathway, giving way to aerobic fermentation. This fermentation yields ethanol which can be further consumed through the respiration pathway, when glucose concentrations reach low levels, leading to a diauxic growth profile.

2.3.3 Parameters for evaluation of growth

In order to evaluate the cell growth, a number of parameters is usually calculated, in order to compare different growth dynamics. Three of these parameters are the lag time, the specific growth rate and the doubling time.

The lag time, as said in section 2.3.1, is the duration of the lag phase and indicates how fast the culture can adapt to new culture conditions.

The specific growth rate is defined as the increase in cell mass per unit time, e.g., grams cells (g) per gram cells (g) per hour (h). The specific growth rate is a way of measuring how fast the cells are dividing in a culture. This leads to the last parameter referred, the doubling time, which is also an indicator of the rate of division of the cells in a culture. It is defined as the time that it takes for a cell to divide and originate one more cell and it is proportional to the inverse of the specific growth rate. It is important to note that these two last parameters can only be calculated during the exponential phase, since it is the growth phase in which most of the cell division takes place.

The detailed explanation for the calculation of these parameters is described in Annex B.

Chapter 3

Materials and Methods

3.1 Materials

3.1.1 Equipment

The equipment used in general laboratory practice is listed on table 3.1.

Table 3.1: Equipment used in general laboratory practice.

Equipment	Supplier	Model
Centrifuge	Sigma	4K15C
	Eppendorf	5415D
	Sorvall	RC5B PLUS
Distillation chiller	Buchi	B-741
Drying cabinet	Memmert	UF 750
Heating bath	Buchi	B-491
HPLC	Agilent Technologies	1260 Infinity
Incubation shaker	Infors	HT Multitron
Magnetic stirrer	IKA	RCT Classic
Photometer	Shimadzu	UV-1800
Rotavapor	Buchi	R-210
Thermoblock	Eppendorf	Thermomixer comfort
Ultracentrifuge	Sorvall	Discovery SE
Vacuum concentrator	Eppendorf	Concentrator Plus Vacufuge Plus
Vacuum controller	Buchi	V-850
Vacuum pump	Buchi	V-700

3.1.2 Chemicals

The chemicals used for preparation of media, stocks and buffers, as well as in general laboratory practice are presented on table 3.2.

Table 3.2: Chemicals used in general laboratory practice.

Chemical	Supplier	Details
Acetonitrile	Sigma-Aldrich	$\geq 99.9\%$ purity
Adenine Hemisulfate	Sigma-Aldrich	$\geq 99\%$ purity
Agar-agar	Carl Roth	
Alanine	Merck	$> 99\%$ purity
p-Aminobenzoic Acid potassium salt	Sigma-Aldrich	$\geq 99\%$ purity
Aspargine Monohydrate	Merck	$> 99\%$ purity
Aspartic Acid	Merck	$> 99\%$ purity
Bactopeptone	Becton, Dickinson & Co.	
Cystein Hydrochloride monohydrate	Sigma	$\geq 98\%$ purity
Dimethylsulphoxide	Fisher	$\geq 99.8\%$ purity
(1,4)-Dithiothreitol	Carl Roth	$\geq 99\%$ purity
Ethanol	Fluka	96% purity
Ethyl Acetate	AppliChem	99.5% purity
Galactose	Carl Roth	$\geq 98\%$ purity
Glucose	Carl Roth	$\geq 99.5\%$ purity
Glutamine	Merck	$> 99\%$ purity
Glycerol	Carl Roth	$> 98\%$ purity
Glycine	AppliChem	$\geq 99.5\%$ purity
Histidine	Carl Roth	$\geq 99\%$ purity
Hydrogen Chloride	Carl Roth	
myo-Inositol	Carl Roth	$\geq 99\%$ purity
Isoleucine	Carl Roth	$\geq 99\%$ purity
Lithium Acetate	Carl Roth	$> 99\%$ purity
Lysine Monohydrochloride	Merck	$> 99\%$ purity
Lyticase	Self-made	$> 99\%$ purity
Magnesium Sulphate	VWR	$\geq 98\%$ purity
Methanol	VWR	99.9% purity
Methionine	Merck	$> 99\%$ purity
Na_2EDTA	Carl Roth	$\geq 99\%$ purity
Olivetol	Sigma-Aldrich	95% purity
Olivetolic Acid	Santa Cruz Biotechnology	96% purity
PEG 3350	Sigma-Aldrich	
Peptone	Fluka	
L-Phenylalanine	AppliChem	$\geq 99.5\%$ purity
Phenylmethylsulfonylfluorid	Carl Roth	$\geq 99\%$ purity
Proline	Carl Roth	$> 98.5\%$ purity
Deoxyribonucleic acid sodium salt from salmon testes (Salmon Sperm DNA)	Sigma-Aldrich	
Serine	Carl Roth	$\geq 99\%$ purity
Threonine	Carl Roth	$\geq 99\%$ purity
Tris	Carl Roth	$\geq 99.3\%$ purity
Tryptophane	AppliChem	99% purity
Uracil	AppliChem	$\geq 99\%$ purity
Valine	Merck	$> 99\%$ purity
Yeast Extract	Carl Roth	
Yeast Nitrogen Base Without Aminoacids	Carl Roth	

3.1.3 Media, Stocks and Buffers

3.1.3.1 Media

- YNB -Leu compound medium

The composition of the 10 x YNB -Leu Compound Media is shown in table 3.3.

Table 3.3: Compounds and respective amounts used for preparation of YNB -Leu compound medium.

Compound	Amount (g)
Yeast nitrogen base w/o amino acids	6.8
Supplements w/o leu, ura [a]	1.546
Uracil	0.076

[a] The composition of the supplements without Leu, Ura is shown in Appendix A.

These amounts were dissolved in ultrapure water to complete a total volume of 100 ml and the resulting solution was filtered sterile through a 0.2 micrometre-pore filter and stored at 4 ^{o}C.

This medium is used only in precultures, not in main cultures. It is a nutrient-rich microbial medium that contains nitrogen, vitamins, trace elements, and salts. It is used to classify *Saccharomyces cerevisiae* in amino acid and carbon requirements. In this case, using this medium in the preculture keeps selective pressure on the plasmid.

- YP medium

  The composition of this medium is shown in table 3.4.

  Table 3.4: Compounds and respective amounts used for preparation of YP medium.

Compound	Amount (g)
Tryptone	20
Yeast Extract	10

  These amounts are dissolved in ultrapure water to complete a total volume of 1 l and the resulting solution is then autoclaved and stored at room temperature.

  This medium is high in carbon content and it is used for the growth of yeast.

- YPD medium

  The composition of this medium is shown in table 3.5.

  Table 3.5: Compounds and respective amounts used for preparation of YPD medium.

Compound	Amount (g)
Peptone	20
Yeast Extract	10
Glucose	20

  These amounts are dissolved in ultrapure water to complete a total volume of 1 l and the resulting solution is then autoclaved and stored at room temperature.

  This medium is high in carbon content and it is used for the growth of yeast.

- Complex culture medium

  The composition of this medium is shown in table 3.6.

Table 3.6: Compounds and respective amounts used for preparation of complex culture medium.

Compound	Amount (g)
Yeast extract	20
Bactopeptone	20

These amounts are dissolved in ultrapure water to complete a total volume of 1 l and the resulting solution is then autoclaved and stored at room temperature.

This medium is high in carbon content and it is used for the growth of yeast.

3.1.3.2 Stocks

The stock solutions used are presented in table 3.7.

Table 3.7: Stock solutions and respective final concentrations and solvents.

Stock Solution	Final Concentration	Solvent
Glucose [a]	40 % (m/v)	Ultrapure water
Galactose [a]	20 % (m/v)	Ultrapure water
Olivetol [b]	500 mM	DMSO
Olivetolic Acid [c]	500 mM	DMSO
Lithium Acetate [d]	1 M	Ultrapure water
PEG MW 3350 [e]	500 g/l	Ultrapure water
Dithiothreitol (DTT) [f]	1 M	Ultrapure water
Phenylmethylsulfonyl Fluoride (PMSF) [f]	100 mM	Isopropanol

[a] This solution must be autoclaved and stored at room temperature.
[b] This solution must be stored at -20 ^{o}C and the Eppendorf cup's lid must be covered with parafilm.
[c] This solution must be stored at -20 ^{o}C in a glass vial.
[d] This solution must be sterilized either by autoclaving or filtering and stored at room temperature.
[e] This solution must be autoclaved and stored at room temperature; the pipetting of this solution should be done carefully, since it is very viscous.
[f] This solution must be stored at -20 ^{o}C.

3.1.3.3 Buffers

- GTEB Buffer

  The compounds used for preparation of this buffer, the respective amounts used and final concentrations are shown in table 3.8.

Table 3.8: Chemicals used for preparation of GTEB Buffer and respective final concentrations and amounts used.

Compound	Final Concentration	Amount
Glycerol	20 %	200 ml
Tris	50 mM	6 g
DTT	5 mM	0.25 ml
PMSF	1 mM	0.5 ml

After adding the Tris to the glycerol, the pH must be corrected to 7.5. Afterwards, water is added to complete a total volume of 1 l. The DTT and the PMSF must be added fresh before each usage. The solution must be stored at 4 ^{o}C.

- TE Buffer

  The compounds and respective amounts used in the preparation of this buffer are shown in table 3.9.

  Table 3.9: Chemicals used for preparation of TE Buffer and amounts used.

Compound	Final concentration (mM)	Amount (g)
Tris	10	1.211
Na_2EDTA	1	0.372

  The pH must be corrected to 8.0 either by adding HCl of NaOH and ultrapure water must be added to complete a total volume of 1 liter, followed by sterilization through autoclaving.

- Frozen Competent Cell (FCC) Solution

  The compounds used for preparation of this buffer and the respective amounts used and final concentrations are shown in table 3.10.

Table 3.10: Chemicals used for preparation of FCC Solution and respective final concentrations and amounts used.

Compound	Final Concentration	Amount
Glycerol	5 % (v/v)	0.5 ml
DMSO	10 % (v/v)	1 ml

  Ultrapure water must be added until completing a total volume of 10 ml, and the resulting solution should be filtered with a 0.2 micrometre-pore filter to sterilize.

3.1.3.4 Strain used

In this work, the only microorganism used is *Saccharomyces cerevisiae*. Being a simple single-cell eukaryote, but at the same time, one of the most studied experimental microorganisms, it is one of the best organisms to use in research. In this case, the exact strain of *Saccharomyces cerevisiae* is the W303-1A.

This specific strain was engineered so that it does not present the gal4 and the pep4 genes (Δgal4 and Δpep4).

Also, the insertion of the plasmid pDIONYSOS with a prenyltransferase (PT1), without signal peptide and without yEGFP was performed in this yeast strain (pDio-PT1 w/o SP w/o yEGFP). Because of this, the peptides obtained after expression of proteins do not contain a signal peptide at the N terminus and no yEGFP at the C terminus. The reason why the signal peptide was removed from this plasmid was because a plant prenyltransferase (PT1) was cloned in here, and in studies conducted by Li et. al [73] and Shen et. al [74], it has been shown that a N terminal signal peptide like the chloroplast transit peptide of PT1 inhibits enzyme activity.

The empty vector pDIONYSOS is a 7028 bp high copy plasmid with a Gal1 promoter and with resistance to ampicillin. It also includes a leu2-d marker and a URA 3 gene, as well as pUC, 2μ and f1 origins [75]. This plasmid's map is represented in figure 3.1.

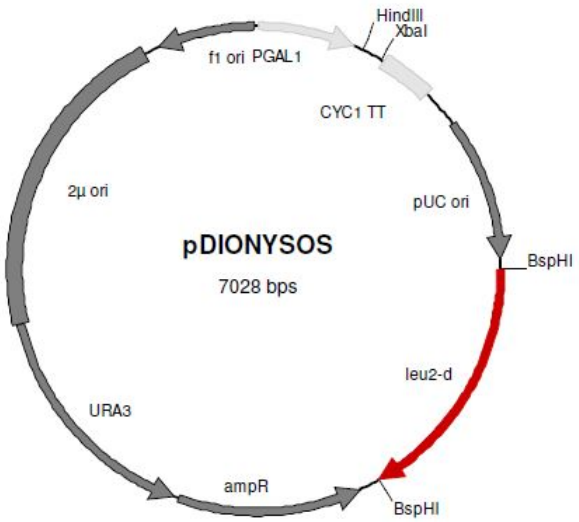

Figure 3.1: Map of the pDIONYSOS plasmid [75].

The empty vector was used in the protocol described in section 3.2.2.3. For the remaining procedures the pDio-PT1 w/o sp w/o yEGFP plasmid was used.

3.2 Methods

3.2.1 Microbiological Methods

3.2.1.1 Cultivation of *Saccharomyces cerevisiae*

For the cultivation of *S. cerevisiae*, before starting the main culture, it is necessary to have two pre-cultures. The first pre-culture must be performed in a baffled flask with a 10 % working volume, with a 2 % (m/v) concentration of glucose, and it must be inoculated from an agar plate containing the desired strain of this yeast. This first pre-culture must be incubated 16 to 24 hours at 30 ^{o}C and 200 rpm.

For the second pre-culture, it is necessary again to have a 2 % concentration of glucose in a 10 % total working volume. The initial OD_{600} should be 0.2 and the incubation should be performed at 200 rpm and 30 ^{o}C for 12 hours.

After these 12 hours, the main culture can be started.

3.2.1.2 Development of a growth curve

In order to build a growth curve, it is necessary to begin with the procedure described in section 3.2.1.1.

Afterwards, two 100 ml cultures are inoculated at the desired initial optical density with 2 % glucose (5 ml glucose 40 %) in YPD medium and two samples are taken from each flask every two hours, until death phase is achieved.

In order to obtain a complete growth curve, other two cultures are inoculated 12 hours after the two first ones with the same conditions and the same procedure is followed.

3.2.1.3 Yeast membrane isolation

The procedure for membrane isolation begins with cell harvesting. For that, the cells are centrifuged at 2000 g for 10 minutes at 4 ^{o}C, followed by a washing step with cold dH_2O. After washing, the pellet is then resuspended in GTEB buffer (1 ml GTEB/g cell mass).

The cells are then transferred to a flask with an appropriate volume, and 300 U/ml of lyticase is added to the cell suspension, which is incubated for at least 70 minutes at 30 ^{o}C and 80 rpm.

After the incubation time, 1 ml of glass beads (0.4 - 0.6 mm) are added per ml of cell suspension in 50 ml Falcon tubes, each filled with a maximum volume of 35 ml. These tubes are then vortexed 10 times for 1 minute at full speed, being placed on ice for 1 minute between each run.

After the last run, the samples are transferred to new Falcon tubes, in order to remove the glass beads and are centrifuged at 4000 g for 20 minutes at 4 ^{o}C. After centrifuging, the supernatant is transferred to a tube for ultracentrifugation at 2.05×10^5 g for 2 hours at 4 ^{o}C. Afterwards, the pellets are resuspended in GTEB buffer (1-2 ml/g of membranes) and the membranes are homogenized using a homogenizer.

3.2.2 Molecular Biology Methods

3.2.2.1 Preparation of Frozen Competent Yeast Cells

The protocol for the preparation of frozen competent *Saccharomyces cerevisiae* cells was adapted from the one written by Gietz and Schiestl [76]. It is briefly described in this section.

The preparation of competent yeast cells begins with a pre-culture with 10 ml YNB -Leu medium (baffled flask, 10 % filling volume) with a few colonies of the desired yeast strain. This culture is incubated for 12 hours at 30 ^{o}C and 200 rpm. After incubation, a 500 ml baffled flask is prepared in order to have a total volume of 50 ml with complex medium and inoculated with an OD_{660} of 0.2, followed by incubation at 200 rpm and 30 ^{o}C. The cells are then harvested at an OD_{660} between 0.5 and 0.6.

This harvesting is performed in 50 ml Falcon tubes through centrifugation at 2000 g for 5 minutes. The cells should then be washed carefully with 25 ml of ultrapure water and centrifuged again for 5 minutes at 2000 g. After centrifuging, the cells should be washed a second time by gently resuspending in 0.5 ml of sterile water and centrifuging 5 minutes at 2000 g after transferring the cell suspension to an Eppendorf cup.

The resulting pellet should be resuspended in 0.5 ml of frozen competent cell solution and the resulting suspension is stored in 50 μl aliquots at -80 ^{o}C in a styrofoam box, in order to freeze it slowly and enhance survival rate. After one night, the box can be removed.

3.2.2.2 Preparation of single-stranded carrier DNA

For the preparation of single-stranded carrier DNA (used in 3.2.2.3), it was necessary to start by dissolving 200 mg of salmon sperm DNA in 100 ml of TE buffer through magnetic stirring at 4 ^{o}C. This procedure can take up to a few hours and one can speed up the dissolution by pipetting the DNA up and down a wide bore 25 ml pipette until no visible DNA is seen.

After dissolution, the resulting solution should be dispensed into 20 samples with 1 ml in 1.5 ml Eppendorf tubes; the remainder volume should be stored in 5 ml samples in 15 ml Falcon tubes. All the samples must be stored at -20 ^{o}C.

Upon usage, the carrier DNA has to be denatured by putting it in a boiling water bath for 5 minutes and chilling it in an ice/water bath before being used.

Note that the denatured carrier DNA can be boiled up to 3 or 4 times without significant loss of activity.

3.2.2.3 Transformation of competent yeast cells

The protocol for the transformation of *Saccharomyces cerevisiae* cells that was followed was the one written by Gietz and Schiestl [76] and it is briefly described in this section.

It is necessary to begin by preparing the following transformation mix (table 3.11):

Table 3.11: Compounds and respective amounts used for preparation of the transformation mix

Compound	**Volume (μl)**
PEG 3350	260
Lithium Acetate	36
Freshly denatured single-stranded carrier DNA (see section 3.2.2.2)	50

Afterwards, it is necessary to resuspend 500 ng of plasmid DNA in 14 μl of sterile dH$_2$O. The competent cells must be thawed at 37 ^{o}C for 15 to 30 seconds and centrifuged for 2 minutes at 13 000 g. After discarding the supernatant, 346 μl of transformation mix are added to the cells and, after adding the 14 μl of DNA, vortex the Eppendorf cups. This is to ensure that there is no pellet on the bottom of the Eppendorf cup and to make sure that the pellet pieces are as small as possible, having in mind that it is not possible to totally ressuspend the pellet. The Eppendorf cups are then incubated for 40 minutes at 42 ^{o}C.

After incubation, the samples were centrifuged for 30 seconds at 13 000 g and the supernatant was discarded. Afterwards, the pellet is resuspended in 200 μl dH$_2$O and the resulting solution is plated directly on a YNB –Ura plate.

After incubation, the cells are harvested and the pellet is ressuspended in 200 μl of dH$_2$O, in order to remove YPD medium totally before plating everything out. This is done in order to select only the cells containing the plasmid. Plates are incubated from 3 to 4 days at 30 ^{o}C. After growing on a YNB -Ura plate, some colonies from this plate are suspended in dH$_2$O and plated out on a YNB -Leu plate and incubated for 2 to 3 days at 30 ^{o}C. This switch from ura marker to leu marker helps increase the copy number of the plasmid in the cells, which is important when expressing membrane proteins like prenyltransferases [77].

After growth of cells, plates should be stored at 4 ^{o}C.

3.2.3 Analytical Methods

3.2.3.1 Evaluating the presence and amount of olivetol and olivetolic acid

The presence of olivetol/olivetolic acid and its abundance in the samples was analysed through High Performance Liquid Chromatography.

The separation of the compound of interest from the remaining compounds is then performed using a Nucleoshell RP 18 column. After this step, the sample goes through a standard UV detector that measures the absorbance against a reference beam and relates its magnitude to the concentration of olivetol/olivetolic acid in the eluent.

The mobile phase used for this method consists in a mixture of water containing 0.1 % of formic acid (mobile phase A) and acetonitrile (mobile phase B) in different proportions (see table 3.12).

The reasons for using a 0.1 % aqueous formic acid solution as mobile phase A are, among others, because a low-pH mobile phase keeps the residual silanol (present in stationary phases) in an undissociated state and, having lower molecular weight than other acids, such as acetic acid and trifluoroacetate, it helps to have a lower interference in the results; also, these added-acids mobile phases are often used in HPLC for analysing basic compounds and formic acid is the acid that is considered to have lower contamination levels for the mobile phase, compared with the acids previously mentioned [78].

The reason for using acetonitrile as mobile phase B and not any other organic solvent, is because this is the organic solvent that keeps the chromatogram's peaks sharper.

The stationary phase of the column (Macherey Nagel NUCLEOSHELL® RP 18) is a core-shell technology silica phase with an octadecyl modification with multi-endcapping, leading to a separation of components based on van der Waals (hydrophobic) interactions. It has a pore size of 90 Angstrom and a carbon content of 7.8 %. It has a particle size of 2.7 μm, a length of 100 mm and a radius of 2 mm.

The HPLC method used for measuring the presence and concentration of olivetol and olivetolic acid is shown in table 3.12.

Table 3.12: Parameters used in the method used for HPLC measurements.

Injected volume of sample	2 μl
Column temperature	40 ^{o}C
Flow	0.7 ml/min
Elution solution	55 % water + 0.1 % FA : 45 % acetonitrile
Wavelength	200 - 400 nm
Duration of run	5 min
Conditions	Isocratic

The following calibration curves were built, in order to convert the area of the peaks in concentrations (see figures 3.2 and 3.3).

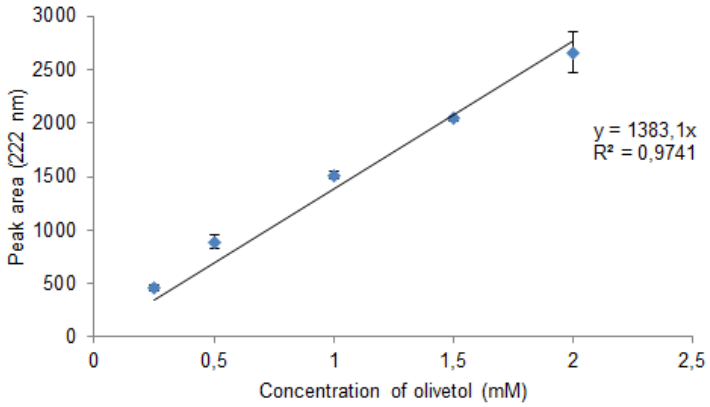

Figure 3.2: Calibration curve for olivetol. Error bars represent standard deviation for n=4.

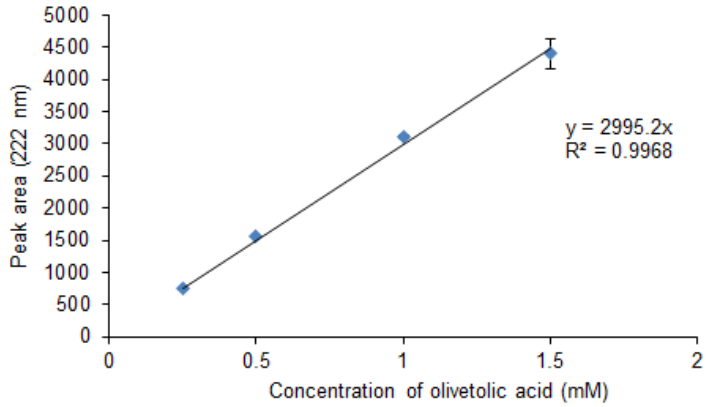

Figure 3.3: Calibration curve for olivetolic acid. Error bars represent standard deviation for n=4.

The softwares used for controlling the chromatography system instruments, for analysing chromatograms and for method setup were, respectively, HyStar, Compass DataAnalysis and otofControl.

3.2.3.2 Determination of Optical Density

The determination of optical density of different cell cultures was done using a spectrophotometer (see Table 3.1) at wavelengths of 600 or 660 nm, diluting the samples to an OD between 0.1 and 0.6, in the linear range of the photometer, in order to follow the Lambert-Beer law.

This technique is based on the turbidity caused by the cells suspended in ultrapure water. A beam of light with the referred wavelength is used to go through the cuvette containing the sample. The relative reduction of the beam's intensity due to the cells suspended is a measure for its concentration (absorbance, A). It is mathematically described by the following equation (3.1):

$$A = log\left(\frac{I_0}{I}\right) \tag{3.1}$$

I_0 represents the intensity of the incoming light, and I represents the intensity of the outgoing light, after going through the cuvette.

3.3 Evaluation of the toxicity of DMSO on *Saccharomyces cerevisiae*

In order to evaluate the toxicity of DMSO, the cell wet weight of the cells was evaluated after cultivation with exposure to different concentrations of DMSO, as well as without any DMSO. The protocol used in this experiment is specific for expression of membrane proteins, since these proteins will eventually need to be expressed simultaneously to the feeding of olivetolic acid.

After incubating the first two pre-cultures with YNB -Leu medium, the main culture was performed in a 500 ml baffled Erlenmeyer flask with a 10 % working volume with complex medium, 2 % (v/v) glucose and 2.8 % (v/v) of absolute ethanol and was inoculated at an OD_{600} of 0.05. This culture was then incubated for 36 hours at 28 ^{o}C and 120 rpm.

After these 36 hours, galactose is added with a final concentration of 2 % (v/v)(5 ml of galactose 20 %) and the DMSO was added in the following concentrations (see table 3.13):

Table 3.13: Concentrations of DMSO used and volumes of DMSO and ultrapure water added to the shaking flasks. Note that two flasks were prepared for each concentration of DMSO tested.

Concentration of DMSO	Volume of DMSO (ml)	Volume of ultrapure water (ml)
0 %	0.0	2.0
1 %	0.5	1.5
2 %	1.0	1.0
3 %	1.5	0.5
4 %	2.0	0.0

After induction, the cultures were incubated for 12 hours at 18 ^{o}C and 120 rpm. After this period, the cultures were induced again with 1 % galactose (2.5 ml galactose 40 %) and incubated for 12 hours at 18 ^{o}C and 120 rpm.

After these 12 hours, the cells were harvested by centrifugation in 50 ml falcon tubes (2000 g, 4 ^{o}C, 10 min), the resulting pellet was washed, it was left upside down for 5 min in order to get rid of as much of the medium as possible and the pellets were then weighed.

3.4 Evaluation of the toxicity of olivetolic acid and olivetol

To evaluate the toxicity of both olivetol and olivetolic acid, a 24-well cell culture plate was prepared with 1 ml of YPD agar in each well, with different concentrations of both olivetol and olivetolic acid being plated out in the agar and, after drying, two different cell suspension concentrations were also plated out (see figure 3.4). The volumes of olivetolic acid and olivetol standard solutions as well as the volumes of the cell suspensions that were plated out were both 20 μl.

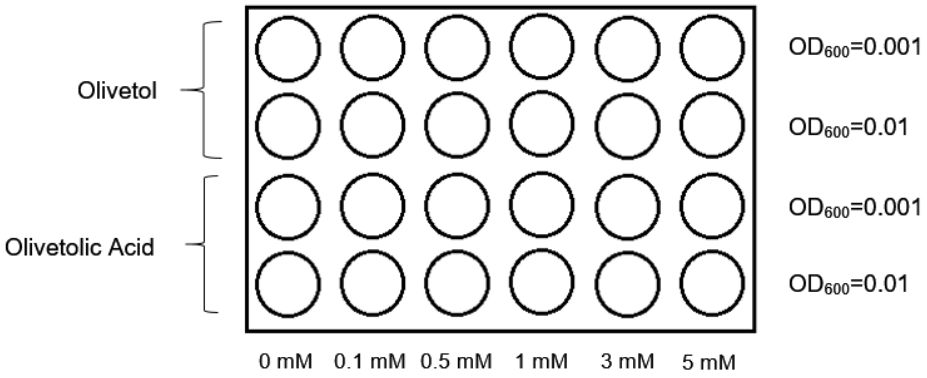

Figure 3.4: Representation of the concentrations of olivetol/olivetolic acid and the concentration of cell suspension plated out in each well of the 24-well cell culture plate.

It is important to note that in order to have always the same percentage (% v/v) of DMSO, the standard solutions plated out were prepared always with the same volume of DMSO. In order to achieve this, prior to the making of the final standard solutions, standard solutions with higher concentrations were prepared from the 500 mM stock solution (see table 3.14).

Table 3.14: Concentration of standard solutions of olivetol/olivetolic acid prepared from the 500 mM stock solution, as well as the volumes of standard solutions and DMSO used, and the final concentration in the wells.

Concentration of standard solution of olivetol/ olivetolic acid (mM)	**Volume of standard solution (μl)**	**Volume of DMSO (μl)**	**Final concentration of olivetol/olivetolic acid in well (mM)**
-	0 [a]	19	0
2	1	19	0.1
10	1	19	0.5
20	1	19	1
60	1	19	3
100	1	19	5

[a] 1 μl of ultrapure water was added instead of olivetol/olivetolic acid.

The plate was incubated at 30 ^{o}C and every 12 hours, a photograph of the 24-well cell culture plate was taken.

3.4.1 Analytical Chemistry Methods

3.4.1.1 Extraction of olivetol/olivetolic acid

The extraction of olivetol and olivetolic acid is performed by adding ethyl acetate in the volumes presented in table 3.15. Different volumes of ethyl acetate were tested for different sample volumes, in order to maximize the extraction efficiency (see section 4.3).

Table 3.15: Optimal volumes of ethyl acetate for different sample volumes.

Volume of sample (ml)	Volume of ethyl acetate (ml)
5	1
1	0.5
0.2	0.2

After adding the respective amount of ethyl acetate for the volume of sample, the sample should be vortexed for one minute, followed by centrifugation at 5000 g for 10 minutes at 4 ^{o}C, in order to allow phase separation. After centrifugation, the upper phase should be transferred into an appropriate container (either an HPLC vial or a receiving flask) for the evaporation of ethyl acetate. On the remaining lower phase, the previous procedure should be repeated two more times. After repeating this procedure, the ethyl acetate is then evaporated from the samples either using a rotavapor or a vacuum concentrator (see table 3.1).

After evaporating the ethyl acetate, the sample is resuspended in 200 μl of methanol (HPLC grade), transferred to an insert in an HPLC vial and analysed through HPLC.

It is important to note that since this organic solvent is prone to leakage, this extraction must be performed either in flasks with screwing caps or in any other flask that doesn't allow leakage, preferrably made of glass - a test tube is ideal.

Chapter 4

Results and Discussion

In this chapter, the main experiments that were performed, as well as the results obtained, will be presented and discussed. First, the toxicity of the solvent used for olivetolic acid and olivetol was tested. On the second place, the toxicity of olivetolic acid and olivetol was evaluated. The next step was building calibration curves for olivetol and olivetolic acid and maximizing the extraction efficiency for these compounds. Also, the effect of olivetol and olivetolic acid on *S. cerevisiae* was evaluated, as well as the possible uptake of olivetol by this organism. Finally, it was tested whether the olivetol accumulates in the membranes or in the cytosol of *Saccharomyces cerevisiae*.

4.1 Evaluation of the toxicity of DMSO on *Saccharomyces cerevisiae*

Since DMSO is the solvent used for both olivetol and olivetolic acid, its influence on the growth behaviour of *Saccharomyces cerevisiae* was studied. Although it has been reported by Bartosz et al [79] that DMSO induces oxidative stress in different strains of yeast, the behaviour of this strain was evaluated, since the maximum concentration used was 4 % (v/v), and there are strains of *S. cerevisiae* reported in this study that were not relevantly influenced with this concentration of DMSO.

The procedure for evaluation of the toxicity of DMSO is described in section 3.2.3.3. The results obtained are presented in figure 4.1:

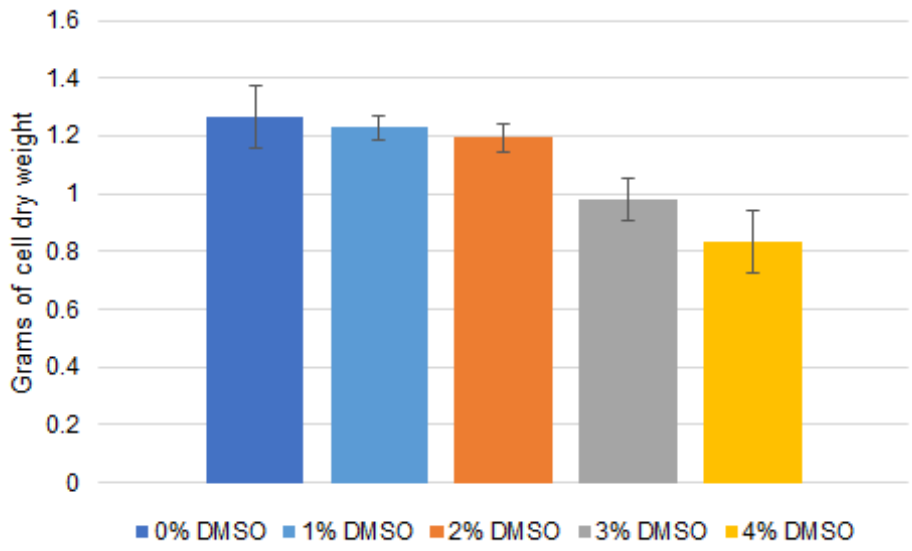

Figure 4.1: Average weight of pellets obtained after exposure to different concentrations of DMSO. Error bars represent the standard deviation for n=2.

The results obtained showed that a higher concentration of DMSO leads to a lower cell weight, leading to believe that this strain of *Saccharomyces cerevisiae* is susceptible to the presence of DMSO. Since DMSO is mainly used as a solvent for substances that are very hard to dissolve, one can assume, that this happens because DMSO solubilizes the membranes of this strain of yeast.

Having this in mind, it is important in further studies to always have the same concentration (% v/v) of DMSO, to make sure that only the presence of olivetolic acid or olivetol are responsible for the different behaviours of *S. cerevisiae* and not the presence of DMSO.

4.2 Optimization of the method used in HPLC

The method initially used, followed the parameters that are presented in table 4.1.

Table 4.1: Parameters used in the first method used for HPLC measurements.

Injected volume of sample	2 μl
Column temperature	35 ^{o}C
Flow	0.7 ml/min
Elution solution	35 % water + 0.1 % FA : 65 % acetonitrile
Wavelength	200 - 400 nm
Duration of run	5 min
Conditions	Isocratic

This method resulted in a chromatogram in which the olivetol peak (blue circle) was overlaid with the injection peak (red circle), as can be seen in figure 4.2.

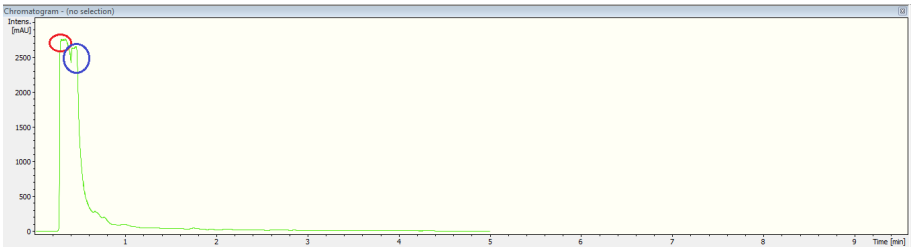

Figure 4.2: Chromatogram of olivetolic acid standard solution analysed with the first HPLC method with injection peak marked with a red circle and with the olivetol peak marked with a blue circle.

In order to increase the retention time of olivetol and olivetolic acid in the column, a new method was tested, in which the temperature was slightly raised and the proportion of the solvents in the elution solution was changed. In this method, the following parameters are used (see table 4.2):

Table 4.2: Parameters used in the second method used for HPLC measurements.

Injected volume of sample	2 μl
Column temperature	40 ^{o}C
Flow	0.7 ml/min
Elution solution	55 % water + 0.1 % FA : 45 % acetonitrile
Wavelength	200 - 400 nm
Duration of run	5 min
Conditions	Isocratic

In order to raise the retention time of olivetol, the temperature was raised to 40 ^{o}C, so that the width of the peak would be lower. Furthermore, the composition of the elution solution was modified to 55 % of water with 0.1 % formic acid and 45 % of acetonitrile. Considering that olivetol and olivetolic acid are organic molecules and show higher affinity to a hydrohobic phase, decreasing the amount of organic phase (acetonitrile) in the elution solution will increase the amount of time that the olivetol/ olivetolic acid will be retained in the column, thus increasing the retention time.

The chromatogram of the same sample, referred to previously and analysed with this new method, is shown in figure 4.3:

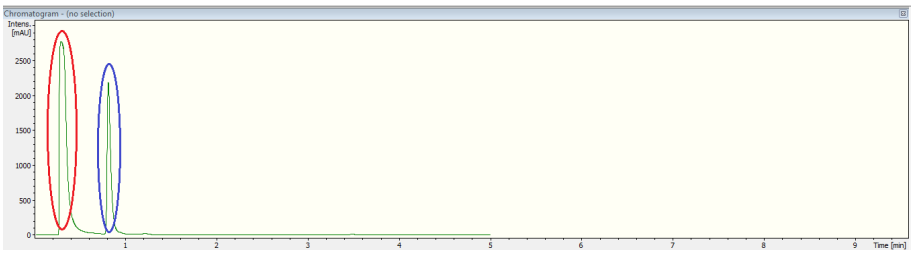

Figure 4.3: Chromatogram of olivetolic acid standard solution analysed with the second HPLC method with injection peak marked with a red circle and with the olivetol peak marked with a blue circle.

Here, the peaks are not overlaid anymore, and the optimization of this method was indeed successful.

4.3 Maximization of olivetol's extraction efficiency

In order to maximize the extraction efficiency of olivetol, samples with different volumes and a known concentration of olivetol (10 mM) were prepared and the extraction procedure was performed with different volumes of ethyl acetate (see table 4.3). For each volume of ethyl acetate tested, four samples with 10 mM olivetol in complex medium were prepared for extraction. The extraction efficiency obtained for each condition is presented in table 4.3:

Table 4.3: Volumes of ethyl acetate tested for extraction of olivetol for each sample volume.

Sample volume (ml)	Volume of ethyl acetate (ml)	Extraction efficiency (%)
5	1	91.0 $\pm$ 6.95
	2.5	90.4 $\pm$ 5.39
1	0.2	80.3 $\pm$ 14.5
	0.5	84.4 $\pm$ 12.5
0.2	0.1	96.0 $\pm$ 3.6
	0.2	96.0 $\pm$ 2.2

For the 0.2 ml samples, higher repeatability was obtained for 0.2 ml of ethyl acetate, and that's the reason why this volume was used and not 0.1 ml.

So, for 5, 1 and 0.2 ml samples, the ethyl acetate volumes used for extraction will be, respectively, 1, 0.5 and 0.2 ml.

4.4 Evaluation of the toxicity of olivetolic acid and olivetol

Considering that the only difference between olivetolic acid and olivetol is the carboxyl group (see figure 4.4), it was assumed that the carboxyl group does not influence the uptake of these compounds and it should not influence the growth behaviour of this strain of *Saccharomyces cerevisiae* either. Nevertheless, the toxicity of both compounds was evaluated.

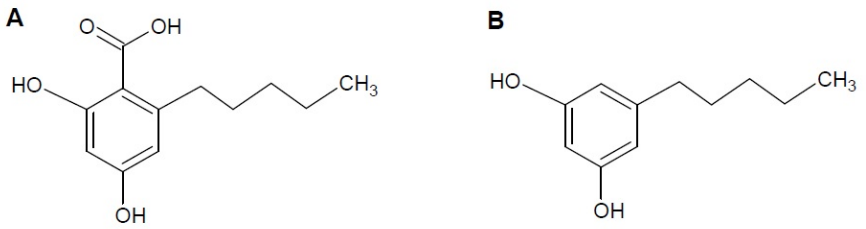

Figure 4.4: Structure of olivetolic acid (A) and olivetol (B).

The procedure for evaluation of the toxicity of olivetol and olivetolic acid is described in section 3.2.3.4. The results are presented in figures 4.5 to 4.10.

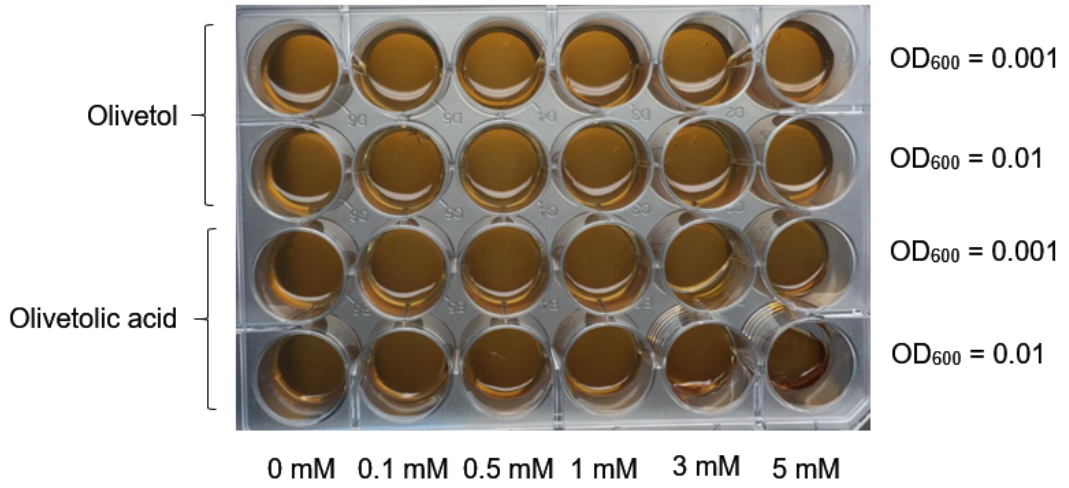

Figure 4.5: 24-well cell culture plate at 0 hours.

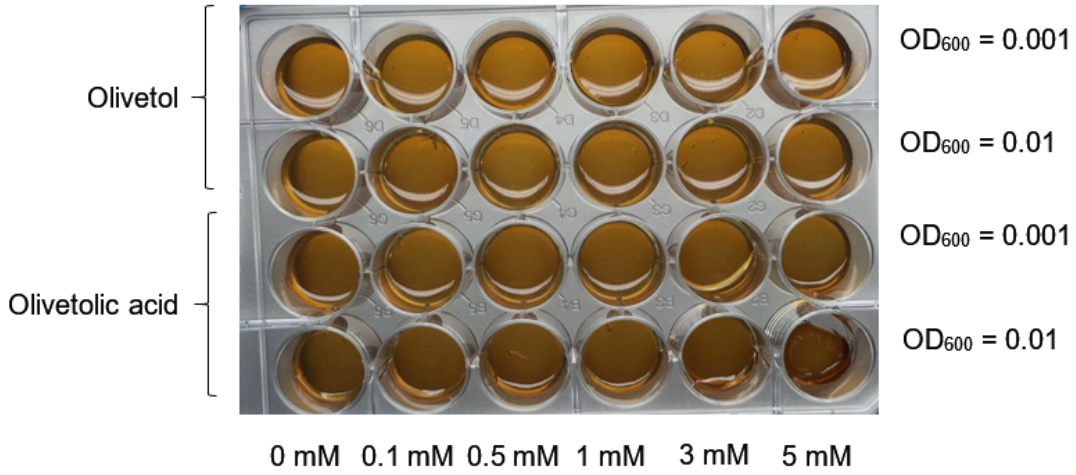

Figure 4.6: 24-well cell culture plate at 12 hours.

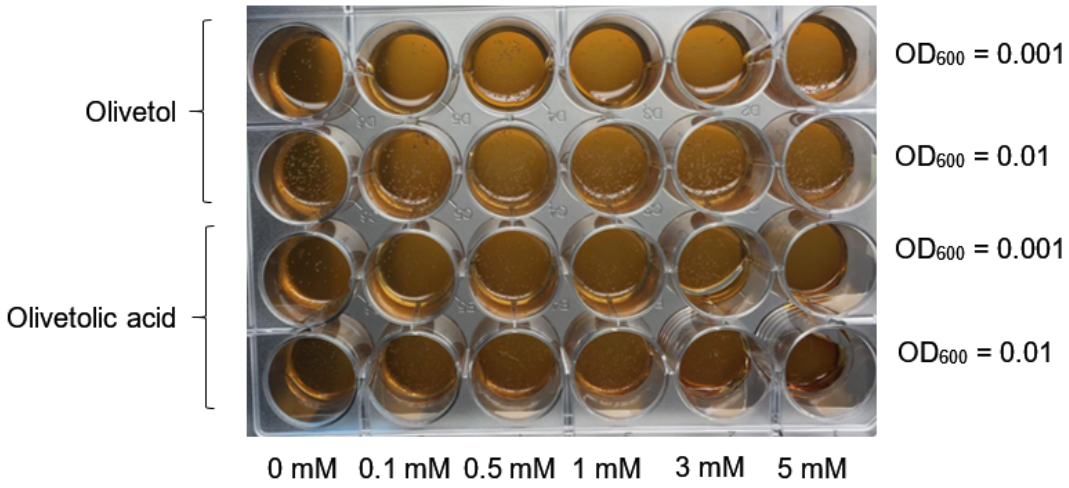

Figure 4.7: 24-well cell culture plate at 24 hours.

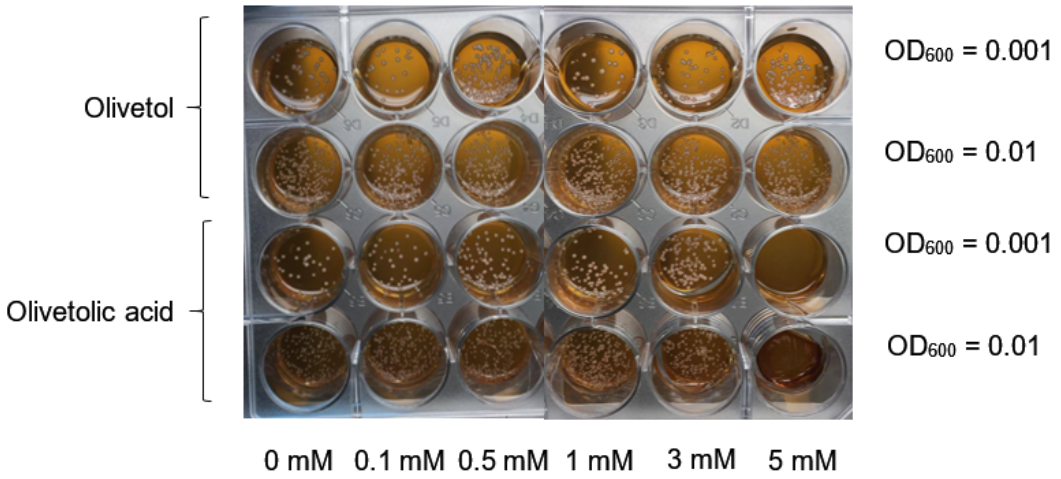

Figure 4.8: 24-well cell culture plate at 36 hours.

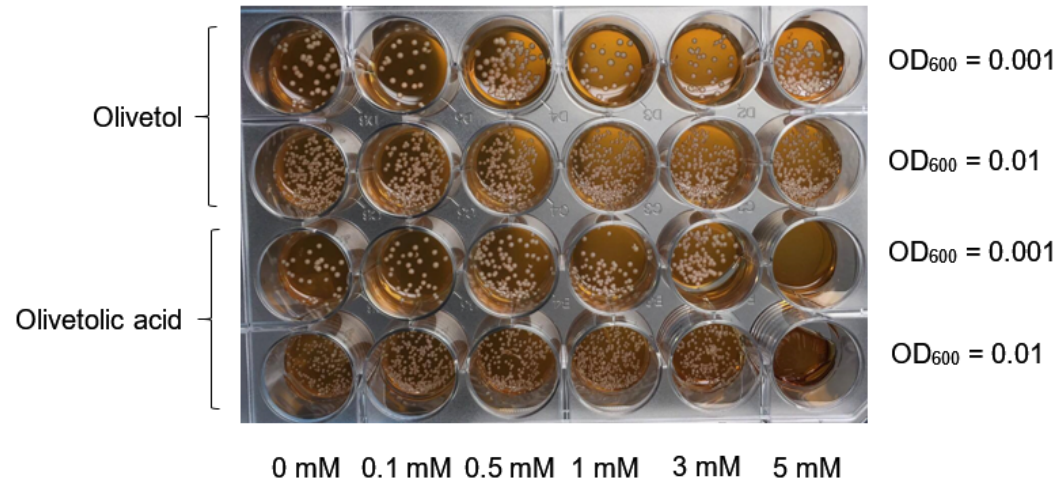

Figure 4.9: 24-well cell culture plate at 48 hours.

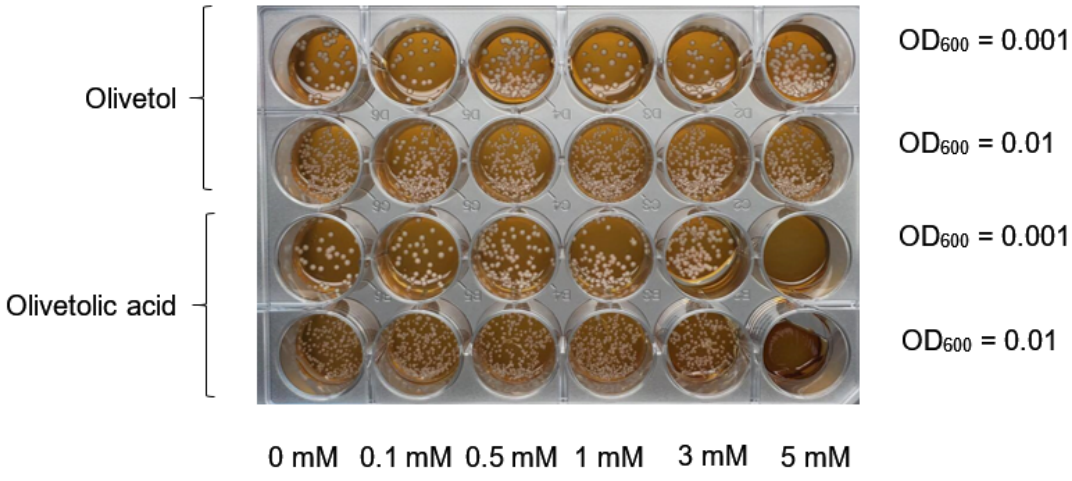

Figure 4.10: 24-well cell culture plate at 60 hours.

It is possible to conclude that, up to a concentration of 3 mM, the growth behaviour of this strain of *Saccharomyces cerevisiae* is identical in both olivetol and olivetolic acid over time, but for a concentration of 5 mM of olivetolic acid, there is an inhibition of its growth. For this reason, the experiments performed further on with olivetol being added to a cell culture didn't have a concentration higher than 3 mM, in order to make sure that olivetol and olivetolic acid didn't reach toxic concentrations.

4.5 Evaluation of the growth profile of this strain of *Saccharomyces cerevisiae* on olivetol

The next step was to study the growth of this strain of *Saccharomyces cerevisiae* in the presence of olivetol to evaluate whether it influences the growth of this yeast. This was achieved by building growth curves under different conditions.

Different starting optical densities and different concentrations of olivetol in the medium were studied, always with a final concentration of DMSO of 1 % (v/v) (see table 4.4):

Table 4.4: Different initial optical densities and final olivetol concentrations for the study of the growth behaviour of this strain of *Saccharomyces cerevisiae*.

Initial OD	Concentration of olivetol (mM)
0.2	0
	0.5
	1
1	0
	0.5
	1

These are the initial OD's tested, since it is the OD's used in the begininng of the yeast cultivation for membrane protein expression.

4.5.1 Growth curves of this strain of *Saccharomyces cerevisiae* with 0 mM olivetol

The growth curves of this strain with initial OD's of 0.2 and 1 with no olivetol are shown in figure 4.11:

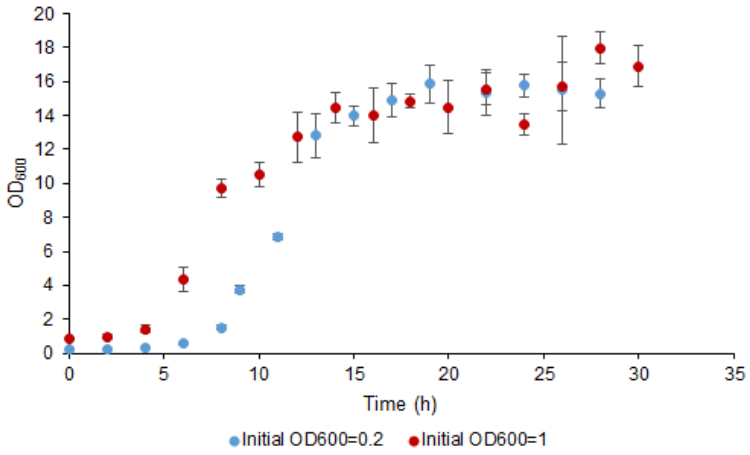

Figure 4.11: Growth curves for this strain of *Saccharomyces cerevisiae* without olivetol and with initial optical densities of 0.2 (blue) and 1 (red). Error bars represent the standard deviation for n=4.

It is possible to see that with higher initial OD, the lag phase tends to be smaller, but the specific growth rate also tends to be lower, leading to a simultaneous start of the stationary phase in both cases.

It is important to note that with higher optical density, samples tend to show higher deviation in this parameter, since this is a strain of yeast used in the brewing industry and it was manipulated so that it would show high flocculation for high cell densities, in order to facilitate the separation process after fermentation.

For the culture with a starting OD of 0.2, the lag time, the specific growth rate and the doubling time were, respectively, 6 h, 0.398 h^{-1} and 1.7 h. Concerning the culture with a starting OD of 1, these parameters assumed 4 h, 0.263 h^{-1} and 2.6 h respectively.

These growth curves are important for comparison of the growth curves with olivetol with reference growth curves.

When building this growth curve, four 200 μl samples were taken at 5, 10, 15 and 20 hours, and run on the HPLC, in order to make sure that there was no signal at the same retention time of the olivetol. The results obtained are represented in figure 4.12 and show that there is indeed no signal at 0.8 min.

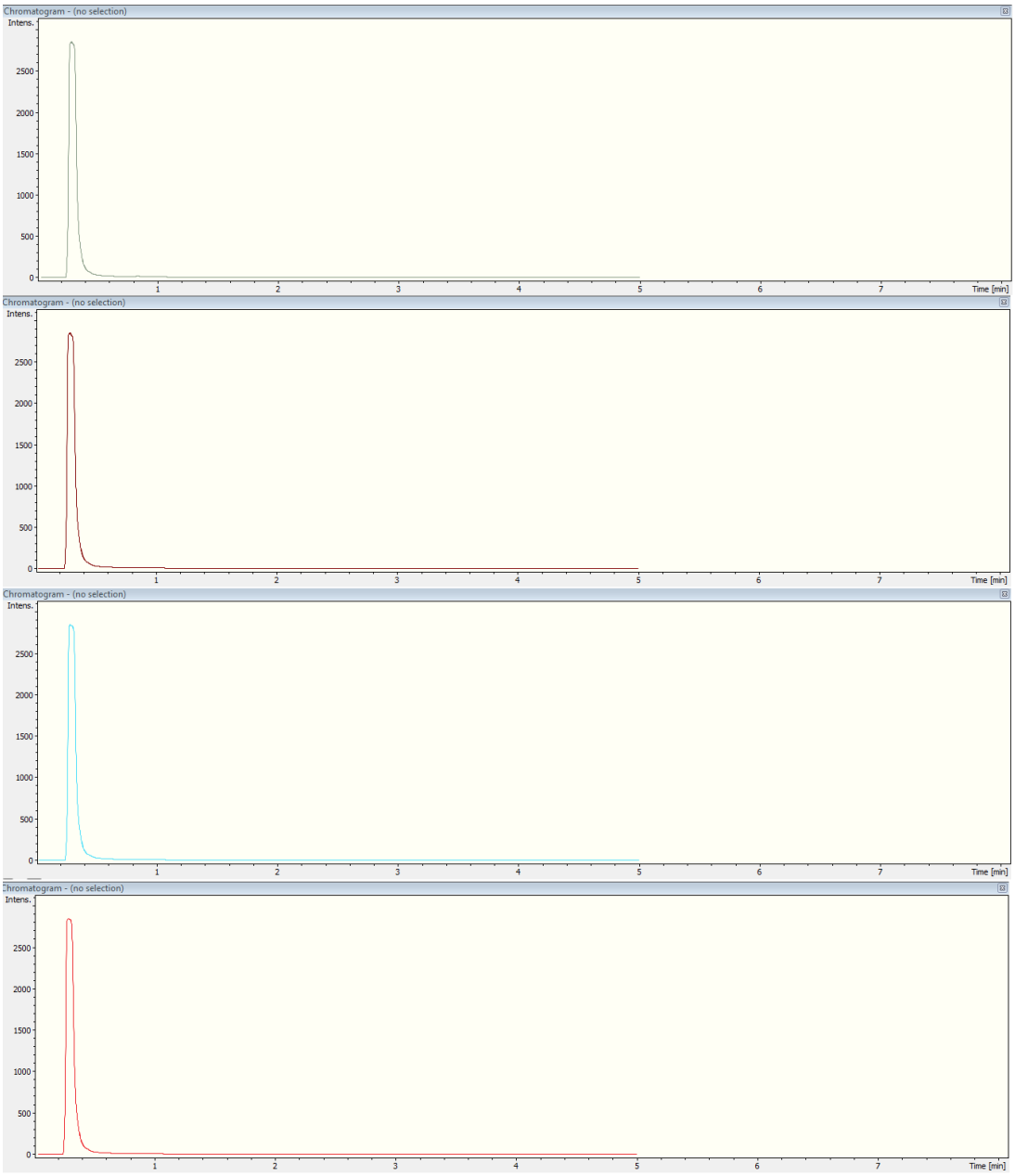

Figure 4.12: HPLC chromatograms of samples without olivetol at 5 (green), 10 (brown), 15 (blue) and 20 (red) hours of cultivation.

4.5.2 Growth curves of this strain of *Saccharomyces cerevisiae* with 0.5 mM olivetol

The growth curves of this strain with initial OD's of 0.2 and 1 with 0.5 mM olivetol are shown in figure 4.13.

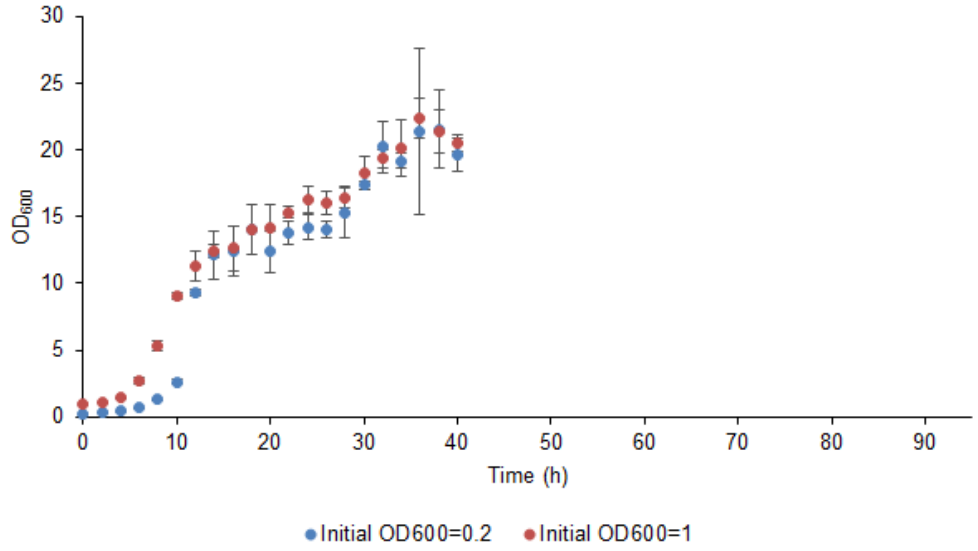

Figure 4.13: Growth curves for this strain of *Saccharomyces cerevisiae* with 0.5 mM olivetol and with initial optical densities of 0.2 (blue) and 1 (red). Error bars represent the standard deviation for n=4.

It is possible to see that in the presence of olivetol, the lag phase tends to be longer than without olivetol, being the exponential phase reached at 10 and 6 hours for initial OD's of 0.2 and 1, respectively. Concerning the specific growth rate, for starting OD's of 0.2 and 1, the values for this parameter were 0.181 and 0.168 h^{-1}, respectively, and the doubling times were 3.8 and 4.1 h, respectively.

Furthermore, it is also possible to see that for different initial OD's, the growth curves show the same profile when exposed to an olivetol concentration of 0.5 mM, as well as when no olivetol is added to the medium, reaching stationary phase simultaneously, even though the lag phase and the specific growth rates are different (see table 4.5).

It is interesting to see that, approximately after 15 hours of achieving stationary phase, the cell culture shows again a slight increase in optical density, almost like a secondary exponential phase. This phenomenon was not further studied, but the most probable explanation is that the cells are showing the Crabtree effect, leading to the production of ethanol in aerobic conditions with excess of glucose in the medium, rather than producing biomass via the tricarboxylic acid cycle. After depletion of glucose, the yeast begins using the ethanol produced as a carbon source, which may explain the second exponential phase. Another plausible hypothesis is that with higher cell density, the olivetol concentration per yeast cell starts to lower, allowing the cell culture to grow under non-inhibiting concentrations.

4.5.3 Growth curves of this strain of *Saccharomyces cerevisiae* with 1 mM olivetol

The growth curves of this strain with initial OD's of 0.2 and 1 and with 1 mM olivetol are shown in figure 4.14:

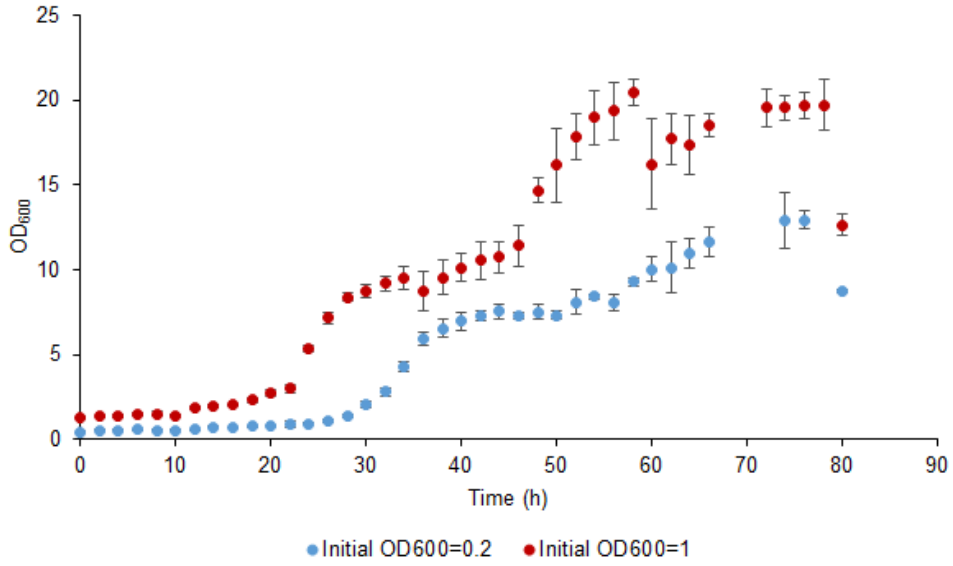

Figure 4.14: Growth curves for this strain of *Saccharomyces cerevisiae* with 1 mM olivetol and with initial optical densities of 0.2 (blue) and 1 (red). Error bars represent the standard deviation for n=4.

Finally, it is possible to verify that with an increasing concentration of olivetol in the medium, this cell culture tends to show an even longer lag phase (30 and 22 hours for initial OD's of 0.2 and 1), when comparing to the growth curves with 0.5 mM of olivetol and with the growth curves without olivetol (see table 4.5). However, in this case, the growth curves with different initial OD's don't seem to reach stationary phase simultaneously. Perhaps the two cultures don't reach the stationary phase simultaneously because this concentration of olivetol already shows a big inhibitory effect for a cell culture with a starting OD of 0.2. Nevertheless, this behaviour should be further studied.

Concerning the specific growth rate, for starting OD's of 0.2 and 1, the values for this parameter was 0.079 and 0.073 h^{-1}, respectively, and the doubling time was 8.8 and 9.5 h, respectively.

Again, two apparent exponential phases are observed in this growth curve, and they occur 15 hours apart from each other, as is the case using 0.5 mM olivetol.

4.5.4 Comparison of growth behaviours under different concentrations of olivetol

The results obtained lead to believe that olivetol has an inhibitory effect on the growth of this strain of *Saccharomyces cerevisiae*. When cell cultures are exposed to an increasing concentration of olivetol, there is a clear tendency to have a longer lag phase, as well as an increasing doubling time and a decreasing specific growth rate (see table 4.5).

Furthermore, with a concentration of 1 mM olivetol, the cell culture with a starting OD of 0.2 does not reach stationary phase simultaneously with the cell culture with an initial OD of 1. This might be another indicator of the inhibitory effect of olivetol in these cell cultures, and it should be further studied.

The main growth parameters were calculated for all growth curves and are shown on table 4.5.

Table 4.5: Main growth parameters calculated for the growth curves obtained for the different conditions tested.

Concentration of olivetol (mM)	**Initial** OD_{600}	**Lag time (h)**	μ **(**h^{-1}**)**	t_d **(h)**
0	0.2	6	0.398	1.7
	1	4	0.263	2.6
0.5	0.2	10	0.181	3.8
	1	6	0.168	4.1
1	0.2	30	0.079	8.8
	1	22	0.073	9.5

4.6 Evaluating the degradation of olivetol in YP medium

It is important to evaluate whether olivetol degrades when added to YP medium, in order to make sure that when having a decrease in its concentration, it is due to a possible upake, and not to its degradation or to a possible reactional modification.

In order to evaluate the degradation of olivetol, olivetol was added to YP medium in 1 liter baffled flasks with a 10 % working volume in two concentrations, 0.5 and 1 mM. These flasks were incubated at 30 ^{o}C and 200 rpm for 70 hours. Two 200 μl samples were taken every 5 hours and the olivetol extraction procedure was performed on those.

The results obtained are shown in figure 4.15.

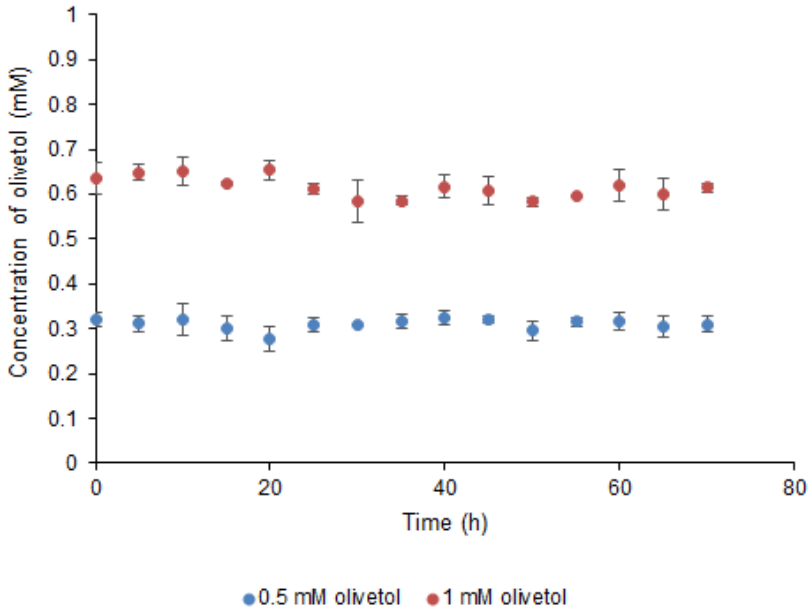

Figure 4.15: Concentration of olivetol over 70 hours in flasks without cell cultures. Error bars represent the standard deviation for n=2.

It is possible to observe that the concentration of olivetol remains unchanged over the 70-hour period, leading to conclude that it does not degrade when in contact with YP medium, as well as when exposed to oxygen and light, at a temperature of 30 ^{o}C.

The concentration in the supernatant seems to be lower than the amount added to the culture medium. This might be due to the olivetol sticking to the plastic in the pipette tips or to the Eppendorf cups. This is a detail that should be further studied. Nevertheless, since this experiment was to evaluate the degradation or modification of olivetol, this does not present a problem.

4.7 Evaluation of the uptake of olivetol/olivetolic acid by this strain of *Saccharomyces cerevisiae*

In order to evaluate if this strain of *S. cerevisiae* can uptake olivetol or olivetolic acid, different approaches were tested.

4.7.1 Evaluating the uptake of olivetol in a 5 ml culture

On this first approach, the main culture is performed in test tubes containing a 5 ml culture with 2 % glucose and 1 mM olivetol in YP medium. These cultures are inoculated at an OD_{600} of 1 and incubated at 30 ^{o}C and 200 rpm. Three 1 ml samples are then collected at six different time points (0, 5, 15, 30, 60 and 120 minutes) and are centrifuged at 5000 g and 4 ^{o}C for 15 minutes, in order to separate the cells from the medium. After this centrifugation, the extraction of olivetol is performed in both pellet and supernatant. The results obtained are presented in figure 4.16:

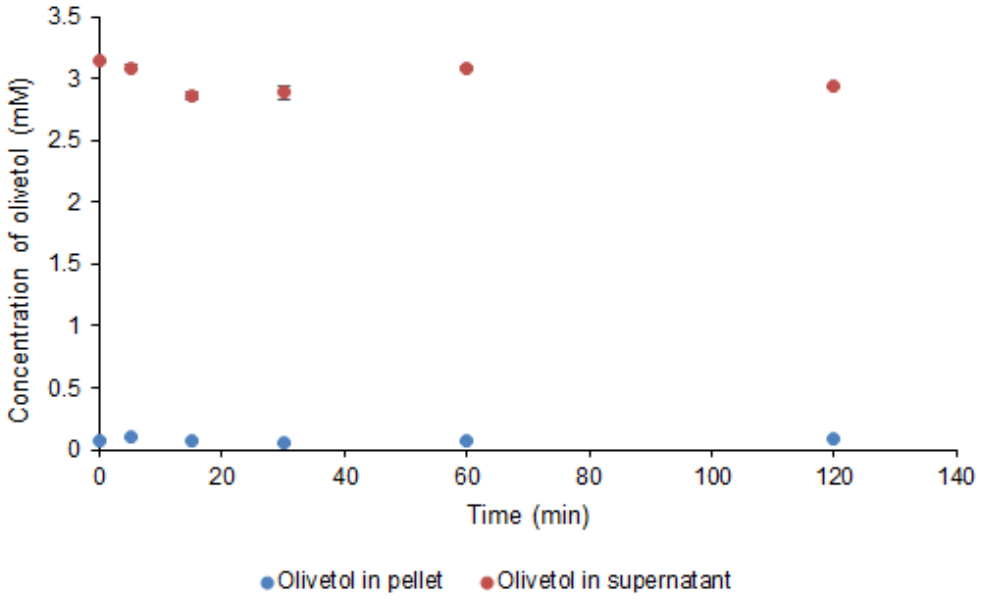

Figure 4.16: Concentration of olivetol in supernatant and in pellet over 2 hours in 5 ml cultures. Note that 1 ml samples are taken and the olivetol present in those samples is ressuspended in 0.2 ml of methanol, hence the average 3 mM concentration on the samples from the supernatant. Error bars represent the standard deviation for n=3.

It is possible to see that the concentration of olivetol in both pellet and supernatant remains unaltered, only with insignificant changes, leading to believe that there was no uptake of olivetol. The residual amounts of olivetol in the pellet might be due to errors associated with the manual separation of pellet and supernatant after centrifugation.

After obtaining these results, it was hypothesized that even though this strain of *Saccharomyces cerevisiae* has the same growth behaviour in both olivetolic acid and olivetol, it might happen that the carboxyl group of olivetolic acid might be essential for its uptake. Therefore, this experiment was repeated with olivetolic acid in a smaller scale. To ensure repeatability, before performing the experiment with olivetolic acid, the same experiment was repeated with olivetol in a smaller scale.

4.7.2 Evaluating the uptake of olivetol in a 1.4 ml culture

To ensure that performing the same experiment in a smaller scale does not influence the results obtained, the same experiment described in section 4.7.1 was repeated in 2 ml Eppendorf cups. Also, in this case, the uptake of olivetol was evaluated over a longer period of time, at 7 different time points (0, 1, 2, 3, 4, 5 and 6 hours), to evaluate if a longer exposure of the cell culture to the olivetol would make a difference in the possible olivetol uptake.

Three 1.4 ml cultures with 2 % glucose and 1 mM olivetol in YP medium were inoculated at an OD_{600} of 1 and incubated at 25 ^{o}C and 1200 rpm in a Thermoblock and a 200 μl sample was taken from each Eppendorf cup at each time point referred previously.

Again, the samples were centrifuged at 5000 g and 4 ^{o}C for 15 minutes, in order to separate the cells from the medium, and the olivetol was extracted from both phases. The results obtained are shown on

figure 4.17:

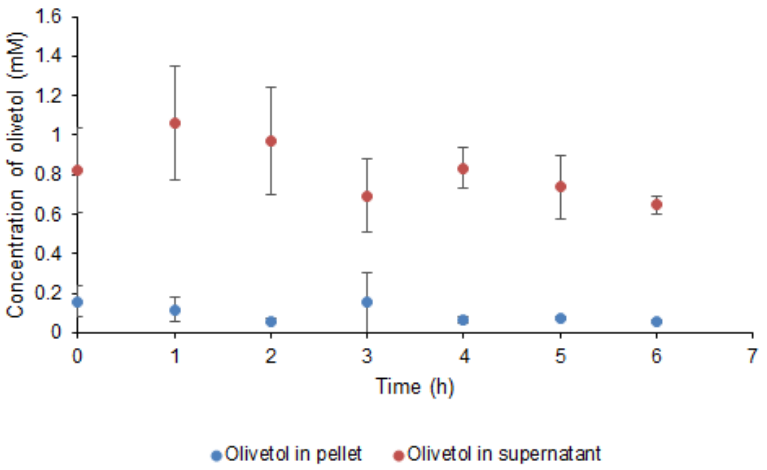

Figure 4.17: Concentration of olivetol in supernatant and in pellet over 6 hours in 1.4 ml cultures. Error bars represent the standard deviation for n=3.

It is possible to conclude that the results obtained are the same. There seems to be no uptake of olivetol over time, even when cells are exposed to it over a longer time period, which leads to the next test performed, the evaluation of the uptake of olivetolic acid.

4.7.3 Evaluating the uptake of olivetolic acid in a 1.4 ml culture

The same experiment described in 4.7.2 was repeated, but this time using olivetolic acid instead of olivetol, to evaluate whether the carboxyl group is important for the uptake of this compound, or not.

The results obtained are shown in figure 4.18:

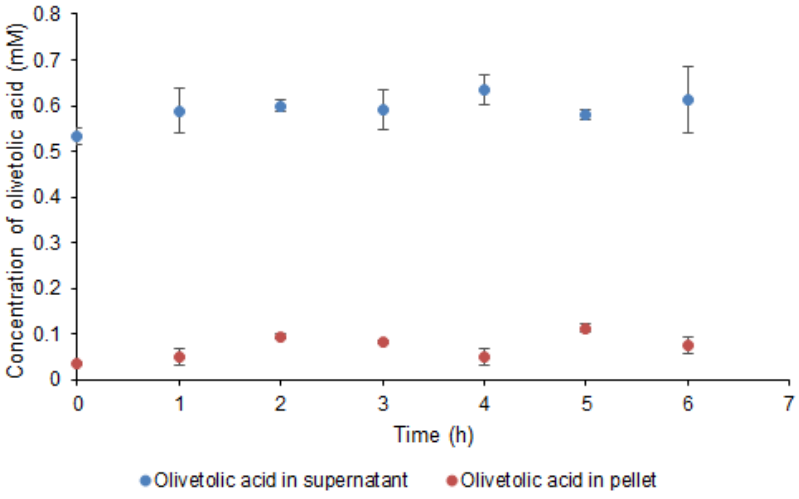

Figure 4.18: Concentration of olivetolic acid in supernatant and in pellet over six hours in 1.4 ml cultures. Error bars represent the standard deviation for n=3.

It is possible to verify that even when using olivetolic acid, there seems to be no uptake over a 6-hour period.

These results lead to the conclusion that the carboxyl group of olivetolic acid is not essential for its uptake by this strain of yeast, and it can be successfully replaced by olivetol.

Again, similarly to the results obtained in section 4.6, there seems to be some loss of olivetol when comparing the concentration in the supernatant and the concentration of olivetol initially in the culture medium. The reason for this behaviour is probably the same, but it should be further studied nevertheless.

Further on, since the same results were obtained with both olivetolic acid and its neutral analogue, olivetol was extracted from both pellet and supernatant, simultaneously to the development of the growth curves with 0, 0.5 and 1 mM olivetol (see sections 4.5.1, 4.5.2 and 4.5.3) every 5 hours until death phase was achieved.

4.7.4 Evaluating the uptake of olivetol in 100 ml cultures

When developing the growth curves described in sections 4.5.2 and 4.5.3, the uptake of olivetol was evaluated over a longer period of time. Two 200 μl samples were taken every 5 hours from each flask, and olivetol was extracted from both pellet and supernatant. For that, the samples were centrifuged at 5000 g and 4 ^{o}C for 15 minutes, in order to separate both phases and the extraction protocol was performed in both of them. The results are shown in sections 4.7.4.1 and 4.7.4.2.

4.7.4.1 Evaluating the uptake of olivetol with 0.5 mM of olivetol

In this section, the evaluation of the uptake of olivetol in 100 ml cultures exposed to 0.5 mM of olivetol and with starting OD's of 0.2 and 1 is described.

The concentration of olivetol in both pellet and supernatant over a 35-hour period is shown in figures 4.19 and 4.20.

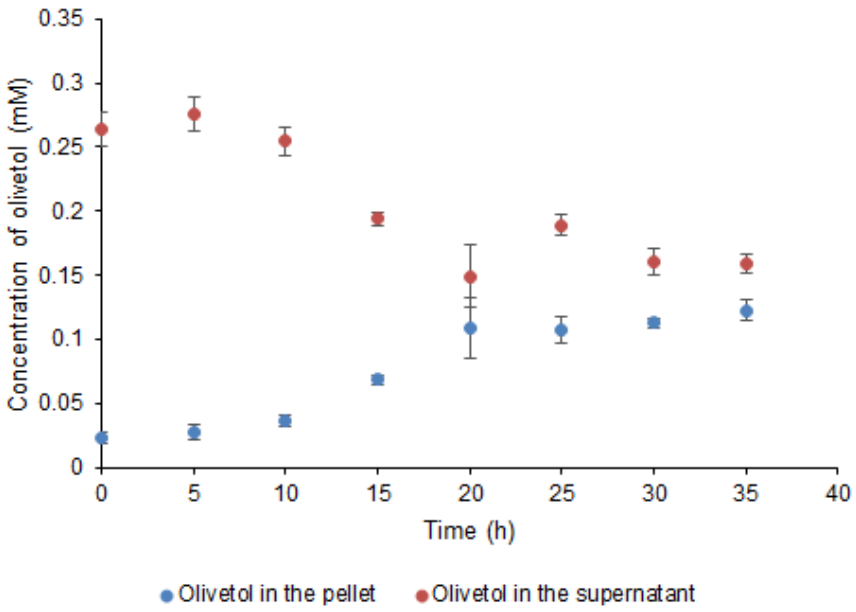

Figure 4.19: Concentration of olivetol in pellet (blue) and in supernatant (red) over time on a culture with a starting optical density of 0.2 and exposed to 0.5 mM of olivetol. Error bars represent the standard deviation for n=3.

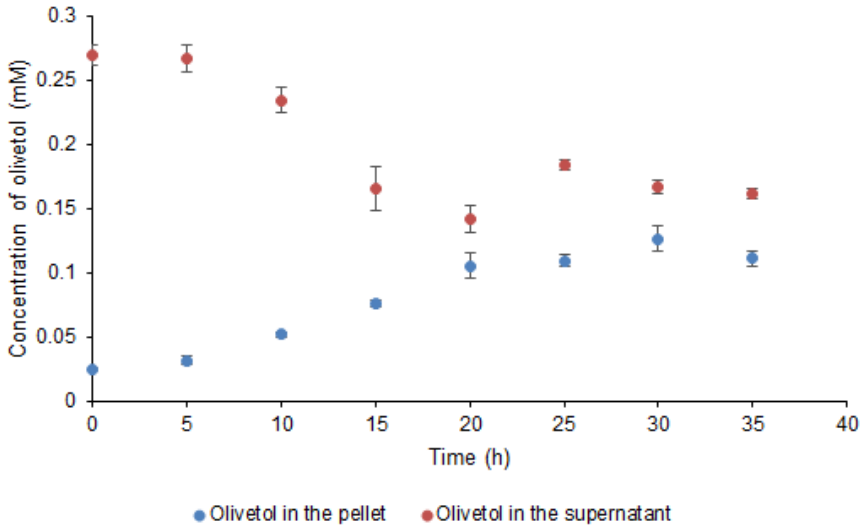

Figure 4.20: Concentration of olivetol in pellet (blue) and in supernatant (red) over time on a culture with a starting optical density of 1 and exposed to 0.5 mM of olivetol. Error bars represent the standard deviation for n=3.

When analysing these results, there seems to be an uptake of olivetol at the 15-hour time point, since the olivetol tends to increase in the pellet and tends to decrease in the supernatant. After this, at the 30-hour time point, this uptake seems to increase, with the amount of olivetol in the pellet and in the supernatant reaching almost identical values.

When comparing these results with the results obtained in section 4.5.2, it is possible to observe that there is a relation between this apparent uptake with the exponential phases observed (see figure 4.21).

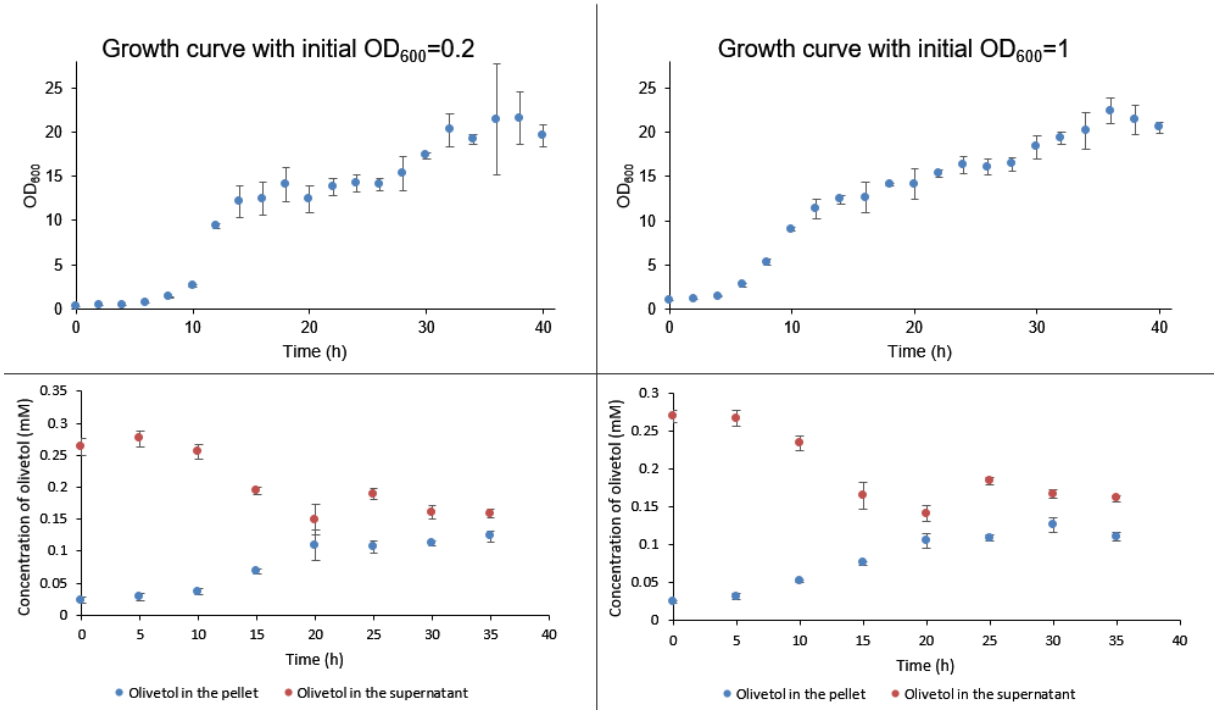

Figure 4.21: Relating the uptake of olivetol with the growth of cell cultures exposed to 0.5 mM of olivetol.

It is possible to see that both stages of the uptake seem to happen simultaneously with the exponential phases of the growth curves. This can indicate that the uptake is related with the duplication of cells, since it is in the exponential phase that the duplication achieves higher rates.

One possible explanation for this is that since olivetol is an organic compound, it has higher affinity for the cell membrane, which is hydrophobic, than for YP medium. So, when cell division takes place, olivetol might be uptaken due to higher affinity with the hydrophobic phase, which in this case is the cell membrane.

Another possibility is that the olivetol is not uptaken, but only adheres to the outer surface of the cell wall and, with higher cell density, the higher the amount of olivetol sticking to this membrane, and the amount of olivetol detected in the medium decreases.

Again, similarly to the results obtained in sections 4.6 and 4.7.2, there seems to be some loss of olivetol when comparing the concentration in the supernatant and the concentration of olivetol initially in the culture medium.

4.7.4.2 Evaluating the uptake of olivetol with 1 mM of olivetol

In this section, the evaluation of the uptake of olivetol in 100 ml cultures exposed to 1 mM of olivetol and with starting OD's of 0.2 and 1 is described.

The concentration of olivetol in both pellet and supernatant over a 80-hour period is shown in figures 4.22 and 4.23.

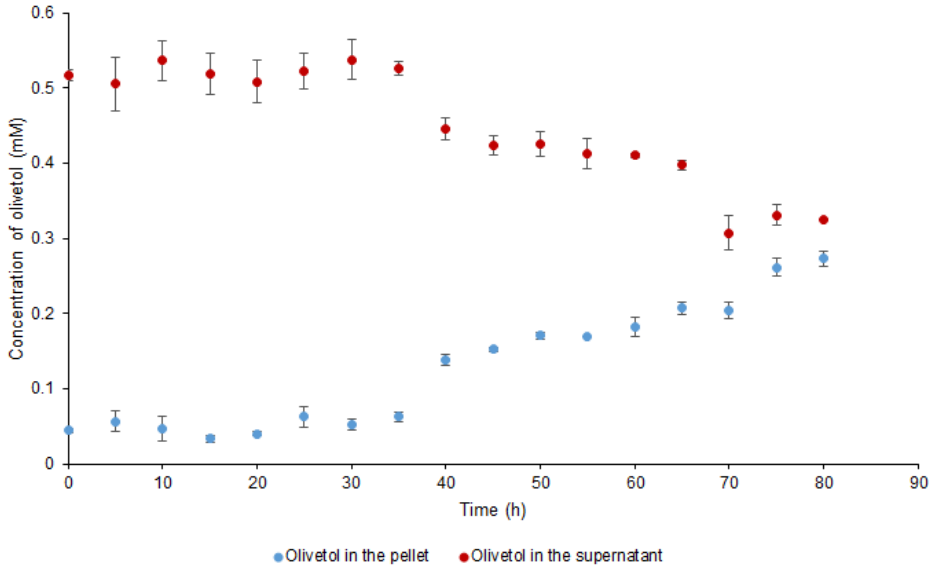

Figure 4.22: Concentration of olivetol in pellet (blue) and in supernatant (red) over time on a culture with a starting optical density of 0.2 and exposed to 1 mM of olivetol. Error bars represent the standard deviation for n=3.

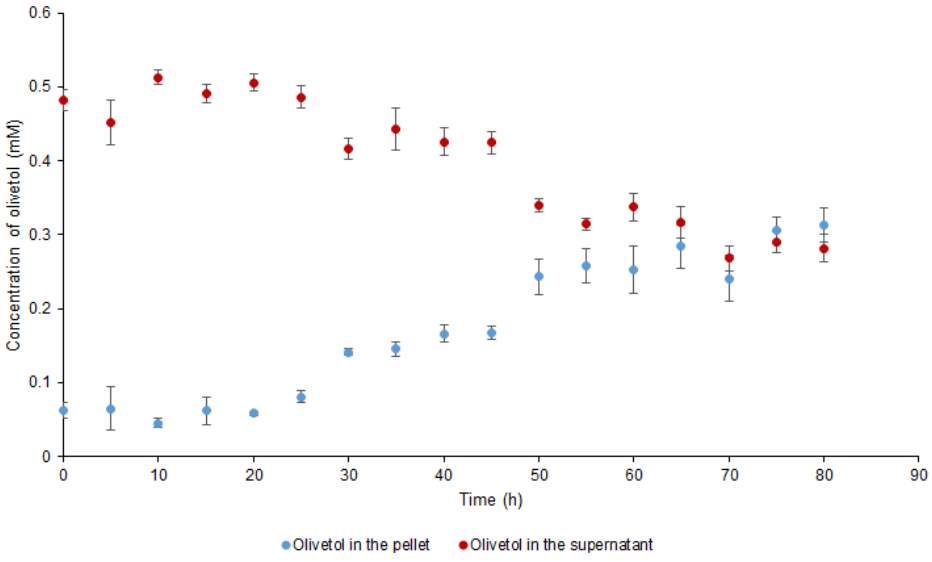

Figure 4.23: Concentration of olivetol in pellet (blue) and in supernatant (red) over time on a culture with a starting optical density of 1 and exposed to 1 mM of olivetol. Error bars represent the standard deviation for n=3.

Again, there seems to be two different time points in the uptake. First, the concentration of olivetol increases in the pellet and decreases in the supernatant at around 40 hours for a starting OD of 0.2 and around 30 hours for a starting OD of 1. The second point is at around 70 hours for a starting OD of 0.2 and at 50 hours for a starting OD of 1. This time point is almost the same as the exponential growth phase in both cases (see figure 4.24), leading to believe that either olivetol might be uptaken due to higher affinity with the cell membrane, than with YP medium, or it adheres to the outer surface of the cell wall.

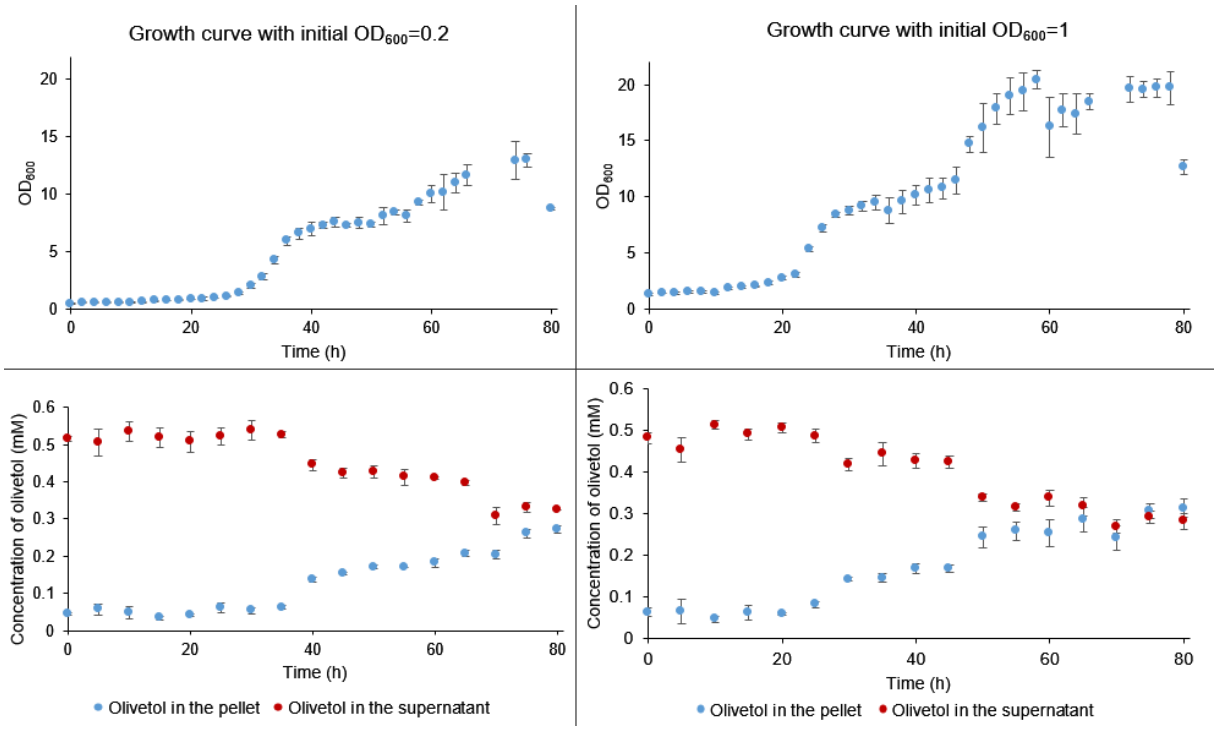

Figure 4.24: Relating the uptake of olivetol with the growth of cell cultures exposed to 1 mM of olivetol.

Again, similarly to the results obtained in sections 4.6, 4.7.2 and 4.7.4.1, there seems to be some loss of olivetol when comparing the concentration in the supernatant and the conentration of olivetol initially in the culture medium.

4.7.4.3 Normalization of the extraction results obtained in 100 ml cultures

In order to normalize these results, the concentration of olivetol in the pellet and in the supernatant was represented at the same cell density (in this case, at an OD_{600} of 10) for all the four different conditions. This representation is shown in figure 4.25.

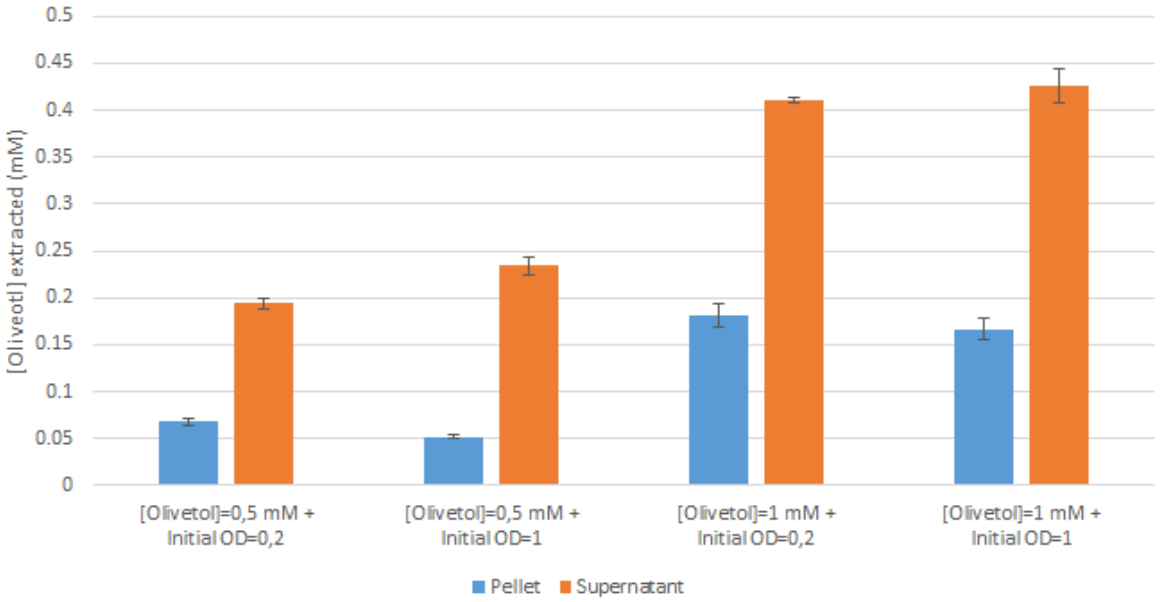

Figure 4.25: Representation of the concentration of olivetol in the pellet and in the supernatant at the same cell density for the different conditions tested (0.5 mM of olivetol and starting OD of 0.2; 0.5 mM of olivetol and starting OD of 1; 1 mM of olivetol and starting OD of 0.2 and 1 mM of olivetol and starting OD of 1). Error bars represent standard deviation for n=3.

It is possible to conclude that the concentrations of olivetol in the pellet and in the supernatant are similar for the same initial concentration of olivetol when initial OD's are different. For a concentration of 1 mM, the amount of olivetol in the pellet is the triple and the amount of olivetol in the supernatant is the double, when comparing with the cultures exposed to 0.5 mM olivetol.

This normalization leads to believe that the hypothesis supporting the adherence of olivetol to the outer surface of the cell wall might be true, since with higher cell density the amount of olivetol in the cell extract is also higher.

So, to evaluate whether the hypothesis of olivetol uptake might also be true, the amount of olivetol uptaken during exponential phases was calculated for the culture exposed to an olivetol concentration of 1 mM, and the results are shown in table 4.6.

Table 4.6: Amount of olivetol uptaken on the first and on the second exponential phases of cultures exposed to 1 mM olivetol and with initial OD's of 0.2 and 1.

	Amount of olivetol uptaken (nmol)	
	First exponential phase	Second exponential phase
Initial OD = 0.2	17	16
Initial OD = 1	16.6	17

It is possible to see that in all the exponential phases for different initial conditions the amount of olivetol that is uptaken is always almost the same (between 16 and 17 nmol), leading to believe that the uptake of olivetol during cell division is also a possible explanation.

4.8 Evaluation of the accumulation site of olivetol

In order to evaluate whether olivetol accumulates in the membrane or in the cytosol of *Saccharomyces cerevisiae*, the procedure for cultivation of *Saccharomyces cervisiae* was followed. After the second preculture reached exponential phase, the cells were harvested by centrifugation at 2000 g and 20 ^{o}C for 10 minutes. After harvesting, the cells were washed and ressuspended in 5 ml ultrapure water and two test tubes with 5 ml cultures were prepared with an OD_{600} of 1 and 2 mM olivetol in YPD medium. These test tubes were then incubated for 48 hours at 30 ^{o}C and 200 rpm. After 48 hours, the protocol for yeast membrane isolation is performed. In the end of this protocol, two solutions are obtained: the homogenized membranes and the supernatant, which contains the membrane proteins as well as the compounds found on the membranes, and the components contained in the cytosol, respectively.

It is important to note that the two final solutions obtained that contain the membrane and the cytosolic extracts show a small volume, but the extraction protocol was performed on it nevertheless.

After performing the extraction protocol on both solutions, the samples were ran on the HPLC and the results obtained are shown in figures 4.26 to 4.29.

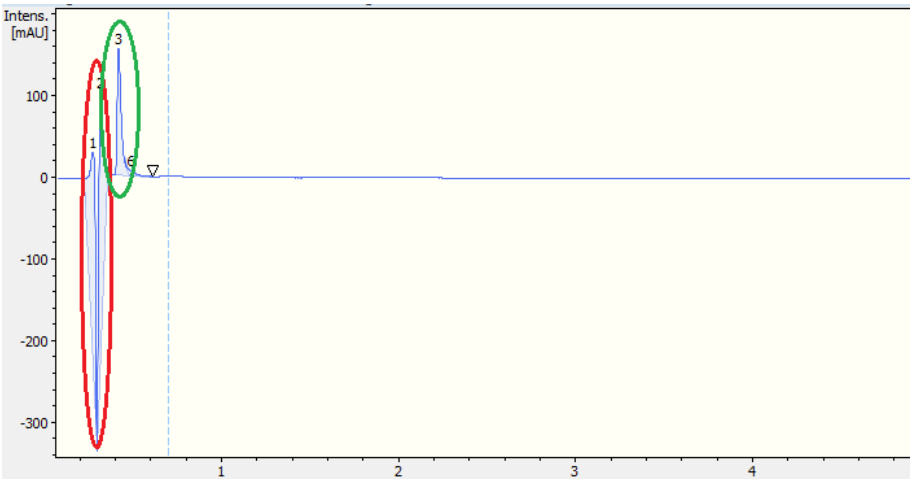

Figure 4.26: HPLC chromatogram of sample I of olivetol extracted from the cytosol of cells. The injection peak is marked with a red circle and the signal peak is marked with a green circle.

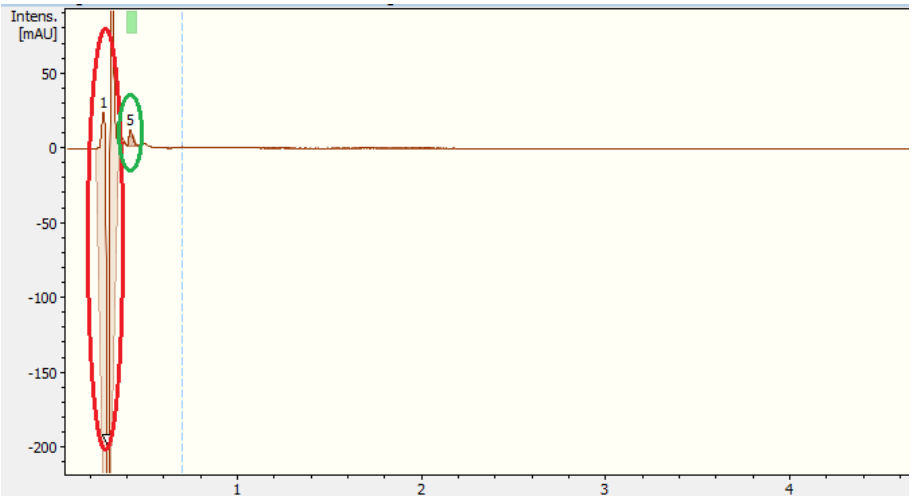

Figure 4.27: HPLC chromatogram of sample II of olivetol extracted from the cytosol of cells. The injection peak is marked with a red circle and the signal peak is marked with a green circle.

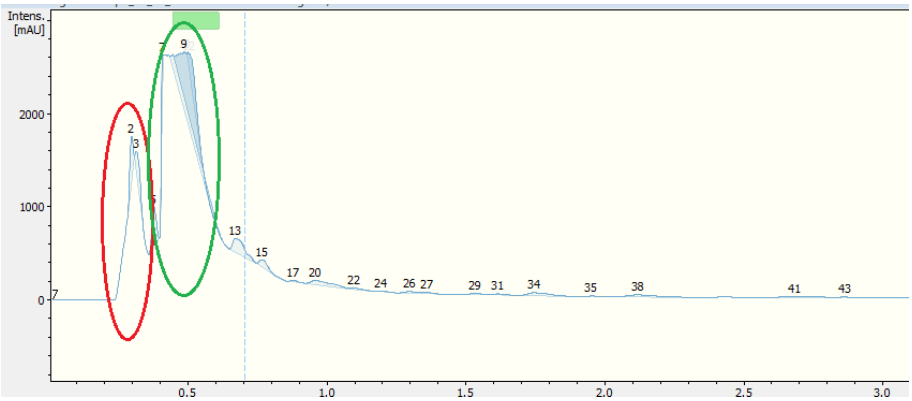

Figure 4.28: HPLC chromatogram of sample I of olivetol extracted from the membranes of cells. The injection peak is marked with a red circle and the overlaid peaks (7 and 9) are marked with a green circle.

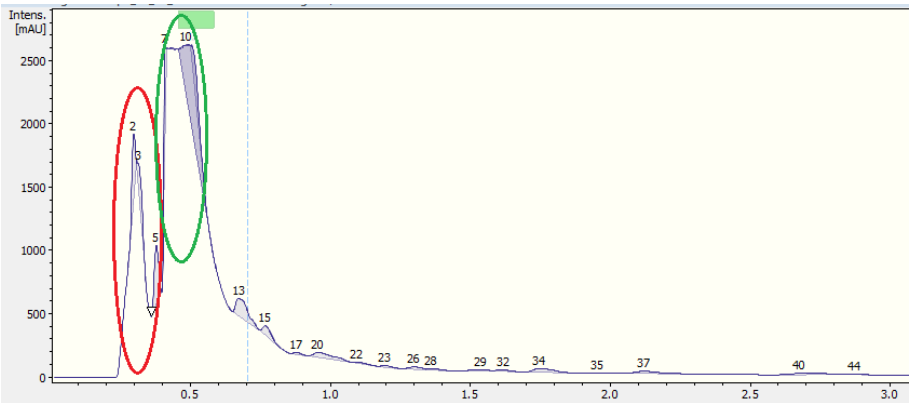

Figure 4.29: HPLC chromatogram of sample II of olivetol extracted from the membranes of cells. The injection peak is marked with a red circle and the overlaid peaks (7 and 10) are marked with a green circle.

These results are inconclusive, since there is an overlay of peaks in figures 4.28 and 4.29, as well as some small signals over time that should be other compounds found in the membranes. Furthermore,

the peaks in figures 4.26 and 4.27 are also very close to the injection peak. Nevertheless, it is possible to see that the peaks in the membrane samples have much higher intensities than the peaks in the cytosol samples. This could indicate that the majority of olivetol is present in the membranes, but no definitive conclusion should be made without further studies.

Chapter 5

Conclusions

In this study, the behaviour of this specific strain of *Saccharomyces cerevisiae* when exposed to different concentrations of olivetol was evaluated, as well as the uptake of olivetol by this strain of yeast. Before that, toxicity tests, as well as tests for maximization of the extraction of olivetol, were conducted. After that, it was evaluated whether the olivetol would accumulate in the membranes or in the cytosol of this organism.

First of all, it was possible to conclude that, for this specific strain of *Saccharomyces cerevisiae*, DMSO is toxic and significant differences in the cell weight can be detected for concentrations higher than 3 % (v/v). Also, it was possible to conclude that olivetolic acid is only toxic to this strain in concentrations higher than 3 mM, but olivetol does not show toxicity for the cells at concentrations up to 5 mM.

Further on, it was concluded that olivetol shows some inhibitory effect on the growth of this strain of yeast, since there is an increase in the lag phase and in the doubling time, as well as a decrease of the specific growth rate, with an increasing concentration of olivetol. It is also possible to see that when olivetol is present during cell growth, the exponential phase is followed by a 15-hour stationary phase, which is then followed by a new exponential phase. The reasons why this happens were not investigated, but the probable explanation is that the cultures are showing the Crabtree effect. Even though it is much less probable, one can also hypothesize that it might happen because the concentration of olivetol per yeast cell decreases in the medium and achieves levels that are no longer toxic, allowing the yeast to grow further.

Even though it seems that there is an uptake of olivetol over time when comparing the growth curves with the olivetol concentration profiles in both pellet and supernatant, the hypothesis of olivetol adhering to the outer surface of the cell wall of this yeast should not be excluded. The normalization of the results was performed in order to exclude one of the hypothesis, but it only showed that both are possible.

5.1 Future Work

To begin with, it would be interesting to study why the yeast cultures show two exponential phases when exposed to olivetol, but not when no olivetol is present in the medium. For that, more parameters should be studied when developing growth curves, such as the pH, ethanol concentration and glucose concentration profiles over time, in order to verify if the effect shown is indeed the Crabtree effect or not.

Furthermore, it would be important to study the growth behaviour of this yeast strain when exposed to a higher concentration of olivetol and with even lower initial optical densities, to see if there is an even higher inhibitory effect. This could explain why the cell cultures with different starting OD's don't reach the stationary phase simultaneouly, when exposed to an olivetol concentration of 1 mM.

Another feature that should be further studied is whether there is an uptake of olivetol or if this compound adheres to the outer surface of this yeast's cell wall. For that, after successful heterologous expression of CBGAS, one could feed olivetolic acid and GPP to yeast cultures and check for CBGA. If CBGA is detected, it is possible to conclude that there is indeed an uptake.

If the hypothesis that supports the uptake of olivetol proves to be true, even if it would make sense that the uptake site would be the membrane, since it is hydrophobic, the uptake site of this compound should be further studied in more detail, either through optimization of the HPLC method that has already been used or even through optimization of the extraction method from the membranes and from the cytosol.

Another trial worth running for the evaluation of the accumulation site of olivetol would be the increase in the culture volume, since it was reported that the volumes of the solutions for extraction were small.

Furthermore, to check if olivetol/olivetolic acid is uptaken into the cell membrane, one can possibly evaluate changes in membrane fluidity. It has been reported that when mammal cells are exposed to drugs and there is an uptake of that drug into the lipid bilayer membrane, there is a significant change in membrane fluidity [80]. Even though the cell type is not the same, both are eukariotic cells with a similar membrane structure. This method could eventually be used to evaluate if there is a drug uptake into the cell membrane.

It has also been reported that the differences in membrane fluidity in different strains of yeast can ease the uptake of toxic compounds [81], so evaluating this uptake in other strains of yeast could be a possibility for future optimization of the uptake of olivetolic acid.

Bibliography

[1] U. N. O. on Drugs and Crime. World Drug Report, 2015.

[2] M. B. Amar. Cannabinoids in medicine: A review of their therapeutical potential. *Journal of Ethno-Pharmacology*, 105:1–25, 2006.

[3] F. Taura, S. Sirikantaramas, Y. Shoyama, Y. Shoyama, and S. Morimoto. Phytocannabinoids in *Cannabis sativa*: Recent studies on biosynthetic enzymes. *Chemistry & Biodiversity*, 4:1649–1663, 2007.

[4] K. Woelkart, O. M. Salo-Ahen, and R. Bauer. Cb receptor ligands from plants. *Curr. Top. Med. Chem*, 8(3):173–186, 2008.

[5] E. Small. Evolution and classification of *Cannabis sativa* (marijuana, hemp) in relation to human utilization. *Bot. Rev.*, 81:189–294, 2015.

[6] D. I. Abrams, J. F. Hilton, R. J. Leiser, S. B. Shade, T. A. Elbeik, F. T. Aweeka, N. L. Benowitz, B. M. Bredt, B. Kosel, J. A. Aberg, S. G. Deeks, T. F. Mitchell, K. Mulligan, P. Becchetti, J. M. McCunne, and M. Schambelan. Short-term effect of cannabinoids in patients with HIV-1 infection, placebo-controlled clinical trial. *Ann. Intern. Med.*, (139):258–266, 2003.

[7] J. E. Beal, R. Olson, L. Laubenstein, J. O. Morales, P. Bellman, B. Yangco, L. Lefkowitz, T. F. Plasse, and K. V. Shepard. Dronabinol as a treatment for anorexia associated with weight loss in patients with AIDS. *J Pain Symptom Manage*, 10(2):89–97, 1995.

[8] A. Jatoi, H. E. Windschitl, C. L. Loprinzi, J. A. Sloan, S. R. Dakhil, J. A. Mailliard, S. Pundaleeka, C. G. Kardinal, T. R. Fitch, J. E. Krook, P. J. Novotny, and B. Christensen. Dronabinol versus megestrol acetate versus combination therapy for cancer-associated anorexia: a North Central Cancer Treatement Group study. *J. Clin. Oncol.*, 20(2):567–573, 2002.

[9] T. S. Herman, L. H. Einhorn, S. E. Jones, C. Nagy, A. B. Chester, J. C. Dean, B. Furnas, S. D. Williams, S. A. Leigh, R. T. Dorr, and T. E. Moon. Superiority of nabilone over prochlorperazine as an antiemetic in patients receiving cancer chemotherapy. *N. Engl. J. Med.*, 300(23):1295–1297, 1979.

[10] A. W. Hutcheon, J. B. Palmer, M. Soukop, D. Cunningham, C. McArdle, J. Welsh, F. Stuart, G. Sangster, S. Kaye, and D. Charlton. A randomized multicentre single blind comparison of a cannabinoid

antiemetic (levonantradol) with chlorpromazine in patients receiving their first cytotoxic chemotherapy. *Eur. J. Cancer Clin. Oncol.*, 19(8):1087–1090, 1983.

[11] J. T. Ungerleider, T. Andrysiak, L. Fairbanks, J. Goodnight, G. Sarna, and K. Jamison. Cannabis and cancer chemotherapy: a comparison of oral delta-9-THC and prochlorperazine. *Cancer*, 50(4): 636–645, 1982.

[12] M. E. Lynch and F. Campbell. Cannabinoids for treatment of chronic non-cancer pain; a systematic review of randomized trials. *Br. J. Clin. Pharmacol.*, 72(5):735–744, 2011.

[13] B. Wilsey, T. Marcotte, R. Deutsch, B. Gouaux, S. Sakai, and H. Donaghe. Low-dose vaporized cannabis significantly improves neuropathic pain. *J. Pain.*, 14(2):136–148, 2013.

[14] B. Wilsey, T. Marcotte, A. Tsodikov, J. Millman, H. Bentley, B. Gouaux, and S. Fishman. A randomized, placebo-controlled, crossover trial of cannabis cigarettes in neuropathic pain. *J. Pain.*, 9(6): 506–521, 2008.

[15] J. Corey-Bloom, T. Wolfson, A. Gamst, S. Jin, T. D. Marcotte, H. Bentley, and B. Gouaux. Smoked cannabis for spascity in multiple sclerosis: a randomized, placebo-controlled trial. *CMAJ*, 184(10): 1143–1150, 2012.

[16] D. J. Rog, T. J. Nurmikko, T. Friede, and C. A. Young. Randomized, controlled trial of cannabis-based medicine in central pain in multiple sclerosis. *Neurology*, 65(6):812–819, 2005.

[17] D. T. Wade, P. Makela, P. Robson, H. House, and C. Bateman. Do cannabis-based medicinal extracts have general or specific effects on symptoms in multiple sclerosis? A double-blind, randomized, placebo controlled study on 160 patients. *Mult. Scler.*, 10(4):434–441, 2004.

[18] L. D. Petrocellis, A. Ligresti, A. Schiano-Moriello, M. Iappelli, R. Verde, C. G. Stott, L. Cristino, P. Orlando, and V. D. Marzo. Non-THC cannabinoids inhibit prostate carcinoma growth in vitro and in vivo: pro-apoptotic effects and underlying mechanisms. *Br. J. Pharmacol*, 168(1):79–102, 2013.

[19] I. Galve-Roperh, C. Sánchez, M. L. Cortés, T. G. del Pulgar, M. Izquierdo, and M. Guzmán. Anti-tumoral action of cannabinoids: involvement of sustained ceramide accumulation and extracellular signal-regulated kinase activation. *Nat. Med.*, 6(3):313–319, 2000.

[20] D. Parolaro and P. Massi. Cannabinoids as potential new therapy for the treatment of gliomas. *Expert Rev. Neurother.*, 8(1):37–49, 2008.

[21] G. Velasco, C. Sánchez, and M. Guzmán. Towards the use of cannabinoids as antitumour agents. *Nat. Rev. Cancer*, 12(6):436–444, 2012.

[22] J. M. Cunha, E. A. Carlini, O. L. Ramos, C. Pimentel, R. Gagliardi, W. L. Sanvito, N. Lander, and R. Mechoulam. Chronic administration of cannabidiol to healthy volunteers and epileptic patients. *Pharmacology*, 21(3):175–185, 1980.

[23] B. E. Porter and C. Jacobson. Report of a parent survey of cannabidiol-enriched cannabis use in pediatric treatment-resistant epilepsy. *Epilepsy Behav.*, 29(3):574–577, 2013.

[24] V. A. Campbell and A. Gowran. Alzheimer's disease; taking the edge off with cannabinoids? *Br. J. Pharmacol.*, 152(5):655–662, 2007.

[25] L. M. Eubanks, C. J. Rogers, A. E. Beuscher, G. F. Koobs, A. J. Olson, T. J. Dickerson, and K. D. Janda. A molecular link between the active component of marijuana and Alzheimer's disease pathology. *Mol. Pharm.*, 3(6):773–777, 2006.

[26] T. Iuvone, G. Esposito, D. D. Filippis, C. Scuderi, and L. Steardo. Cannabidiol: a promising drug for neurodegenerative disorders? *CNS Neurosci. Ther.*, 15(1):65–75, 2009.

[27] O. Sagredo, M. R. Pazos, S. Valdeolivas, and J. Fernandez-Ruiz. Cannabinoids: novel medicines for the treatment of Huntington's disease. *Recent Pat. CNS Drug Discov.*, 7(1):41–48, 2012.

[28] E. A. Penner, H. Buettner, and M. A. Mittelman. The impact of marijuana use on glucose, insulin and insulin resistance among US adults. *Am. J. Med.*, 126(7):583–589, 2013.

[29] L. Weiss, M. Zeira, S. Reich, M. Har-Noy, R. Mechoulam, S. Slavin, and R. Gallily. Cannabidiol lowers incidence of diabetes in non-obese diabetic mice. *Autoimmunity*, 39(2):143–151, 2006.

[30] K. R. Müller-Vahl, U. Schneider, H. Prevedel, K. Theloe, H. Kolbe, T. Daldrup, and H. M. Emrich. Delta 9-tetrahydrocannabinol (THC) is effective in the treatment of tics in Tourette syndrome: a 6-week randomized trial. *J. Clin. Psychiatry*, 64(4):459–465, 2003.

[31] K. R. Müller-Vahl, U. Schneider, A. Koblenz, M. Jöbges, H. Kolbe, T. Daldrup, and H. M. Emrich. Treatment of Tourette's syndrome with Delta 9-tetrahydrocannabinol (THC): a randomized crossover trial. *Pharmacopsychiatry*, 35(2):57–61, 2002.

[32] F. Grotenhermen and E. Russo. *Cannabis and Cannabinoids: Pharmacology, Toxicology and Therapeutic Potential*. 2002.

[33] P. Consroe. Brain cannabinoid systems as targets for the therapy of neurological disorders. *Neurobiol. Dis.*, 5(6):534–551, 1998.

[34] A. A. Izzo, F. Borrelli, R. Capasso, V. D. Marzo, and R. Mechoulam. Non-psychotropic plant cannabinoids: new therapeutic opportunities from an ancient herb. *Trends Pharmacol. Sci.*, 30(10):515–527, 2009.

[35] J. M. McPartland and E. B. Russo. Cannabis and cannabis extracts: greater than the sum of their parts? *J. Cannabis Ther.*, 3/4:103–132, 2001.

[36] R. Mechoulam, L. A. Parker, and R. Gallily. Cannabidiol: an overview of some pharacological aspects. *J. Clin. Pharmacol.*, 42(11):11S–19S, 2002.

[37] C. J. Morgan, R. K. Das, A. Joye, H. V. Curran, and S. K. Kamboj. Cannabidiol reduces cigarette consumption in tobacco smokers: preliminary findings. *Addict. Behav.*, 38(9):2433–2436, 2013.

[38] B. K. Colasanti. A comparison of the ocular and central effects of delt 9-tetrahydrocannabinol and cannabigerol. *J. Ocul. Pharmacol.*, 6(4):259–269, 1990.

[39] F. Borrelli, I. Fasolino, B. Romano, R. Capasso, F. Maiello, D. Coppola, P. Orlando, G. Battista, E. Pagano, V. D. Marzo, and A. A. Izzo. Beneficial effect of the non-psychotropic plant cannabinoid cannabigerol on experimental inflammatory bowel disease. *Biochem. Pharmacol.*, 85(9):1306–1316, 2013.

[40] L. D. Petrocellis, V. Vellani, A. Schiano-Moriello, P. Marini, P. C. Magherini, P. Orlando, and V. D. Marzo. Plant-derived cannabinoids can modulate the activity of transient receptor otent channels of ankyrin type-1 and melastatin type-8. *J. Pharmacol. Exp. Ther.*, 325(3):1007–1015, 2008.

[41] S. Maione, F. Piscitelli, L. Gatta, D. Vita, L. D. Petrocellis, E. Palazzo, V. de Novellis, and V. D. Marzo. Non-psychoactive cannabinoids modulate the descending pathway of antinociception in anaesthetized rats through several mechanisms of action. *Br. J. Pharmacol.*, 162(3):584–596, 2011.

[42] N. Shinjyo and V. D. Marzo. The effect of cannabichromene on adult neural stem/progenitor cells. *Neurochem. Int.*, 63(5):432–437, 2013. doi: 10.1016/j.neuint.2013.08.002.

[43] A. A. Izzo, R. Capasso, G. Aviello, F. Borrelli, B. Romano, F. Piscitelli, L. Gallo, F. Capasso, P. Orlando, and V. D. Marzo. Inhibitory effect of cannabichromene, a major non-psychotropic cannabinoid extracted from *cannabis sativa*, on inflammation-induced hypermotility in mice. *Br. J. Pharmacol.*, 166(4):1444–1460, 2013.

[44] W. M. Davis and N. S. Hatoum. Neurobehavioural actions of cannabichromene and interactions with δ9-tetrahydrocannabinol. *Gen. Pharmac.*, 14(2):247–252, 1983.

[45] T. Yamauchi, Y. Shoyama, H. Aramaki, T. Azuma, and I. Nishioka. Tetrahydrocannabinolic acid, a genuine substance of tetrahydrocannabinol. *Chem. Pharm. Bull.*, 15(7):1075–1076, 1967.

[46] M. Fellermeier and M. H. Zenk. Prenylation of olivetolate by a hemp transferase yields cannabigerolic acid, the percursor of tetrahydrocannabinol. *FEBS Letters*, 427:283–285, 1998.

[47] W. A. Devane, L. Hanus, A. Breuer, R. G. Pertwee, L. A. Stevenson, G. Griffin, D. Gibson, A. Mandelbaum, A. Etinger, and R. Mechoulam. Isolation and structure of a brain constituent that binds to the cannabinoid receptor. *Science*, 258(5090):1946–1949, 1992.

[48] P. Pacher, S. Bátkai, and G. Kunos. The endocannabinoid system as an emerging target of pharmacotherapy. *Pharmacological Reviews*, 58(3):389–461, 2006.

[49] R. K. Razdan. *The Total Synthesis of Cannabinoids*. 1981.

[50] L. Crombie, R. Ponsford, A. Shani, Y. B, and R. Mechoulam. Hashish components. photochemical production of cannabicyclol from cannabichromene. *Tetrahedron Letters*, 9:5771–5772, 1968.

[51] R. Razdan, A. J. Puttick, B. A. Zitko, and G. R. Handrick. Hashish VI: Conversion of (-)-$\delta^{1(6)}$-tetrahydrocannabinol to (-)-$\delta^{1(7)}$-tetrahydrocannabinol. Stability of (-)-δ^{1} and (-)-$\delta^{1(6)}$-tetrahydrocannabinols. *Experientia*, 28:121–122, 1972.

[52] M. Fellermeier, W. Eisenreich, A. Bacher, and M. H. Zenk. Biosynthesis of cannabinoids - incorporation experiment with 13c-labeled glucoses. *Eur. J. Biochem.*, 268:1596–1604, 2001.

[53] W. Eisenreich, A. Bacher, D. Arigoni, and F. Rohdich. Biosynthesis of isoprenoids via the non-mevalonate pathway. *Cell. Mol. Life Sci.*, 61(12):1401–1426, 2004.

[54] C. C. Burke, M. R. Wildung, and R. Croteau. Geranyl diphosphate synthase: cloning, expression and characterization of this prenyltransferase as a heterodimer. *PNAS*, 96(23):13062–13067, 1999.

[55] M. D. Marks, L. Tian, J. P. Wenger, S. N. Omburo, W. Soto-Fuentes, J. He, D. R. Gang, G. D. Weibeln, and R. A. Dixon. Identification of candidate genes affecting δ9-tetrahydrocannabinol biosynthesis in *Cannabis sativa*. *Journal of Experimental Botany*, 60(13):3715–3726, 2009.

[56] J. M. Stout, Z. Boubakir, S. J. Ambrose, R. W. Purves, and J. E. Page. The hexanoyl-CoA percursor for cannabinoid biosynthesis formed by an acyl-activating enzyme in *Cannabis sativa* trichomes. *The Plant Journal*, 71:353–365, 2012.

[57] F. Taura, S. Tanaka, C. Taguchi, T. Fukamizu, H. Tanaka, Y. Shoyama, and S. Morimoto. Characterization of olivetol synthase, a polyketide synthase putatively involved in cannabinoid biosynthetic pathway. *FEBS Letters*, 583:2061–2066, 2009.

[58] S. J. Gagne, J. M. Stout, E. Lui, Z. Boubakir, S. M. Clark, and E. Page. Identification of olivetolic acid cyclase from *Cannabis sativa* reveals a unique catalytic route to plant polyketides. *PNAS*, 109 (31):12811–12816, 2012.

[59] E. P. M. de Meijer, K. M. Hammond, and A. Sutton. The inheritance of chemical phenotype in *Cannabis sativa* L. (IV): cannabinoid-free plants. *Euphytica*, 168:95–112, 2009.

[60] J. Page and Z. Boubakir. Aromatic prenyltransferase from cannabis, 2012. URL `https://www.google.com/patents/US20120144523`. US Patent App. 13/389,815.

[61] S. Morimoto, K. Komatsu, F. Taura, and Y. Shoyama. Enzymological evidence for cannabichromenic acid biosynthesis. *J. Nat. Prod*, 60(8):854–857, 1997.

[62] F. Taura, S. Morimoto, and Y. Shoyama. First direct evidence for the mechanism of δ1-tetrahydrocannabinolic acid. *Journal of the American Chemical Society*, 117:9766–9767, 1995.

[63] F. Taura, S. Morimoto, and Y. Shoyama. Purification and characterization of cannabinolic-acid synthase from *Cannabis sativa* L. *The Journal of Biological Chemistry*, 271(29):17411–17416, 1996.

[64] S. Sirikantaramas, F. Taura, Y. Tanaka, Y. Ishikawa, S. Morimoto, and Y. Shoyama. Tetrahydrocannabinolic acid synthase, the enzyme controlling marijuana psychoactivity, is secreted into the cavity of the glandular trichomes. *Plant Cell Physiol.*, 46(9):1578–1582, 2005.

[65] A. Krivoruchko and J. Nielsen. Production of natural products through metabolic engineering of *Saccharomyces cerevisiae*. *Current Opinion in Biotechnology*, 35:7–15, 2015.

[66] O. W. Richards. The groth of the yeast *Saccharomyces cerevisiae*. I. The growth curve, its mathematical analysis and the effect of temperature on the yeast growth. *Annals of Botany*, 42(165): 271–283, 1928.

[67] P. Held. *Monitoring Growth of Beer Brewing Strains of Saccharomyces Cerevisiae.*, 2010.

[68] M. M. Fonseca and J. A. Teixeira. *Reactores Biológicos: fundamentos e aplicações*. 2007.

[69] M. Lemoigne, J. P. Aubert, and J. Millet. La production d'alcool et le rendement de croissance de la levure de boulangerie cultivée en aérobiose. *Ann. Inst. Pasteur*, 87(427), 1954.

[70] C. Schiraldi, A. Davino, A. Ruggiero, K. D. Corte, and M. D. Rosa. *Saccharomyces pastorianus* as cell factory to improve production of fructose 1,6-diphosphate using novel fermentation strategies. *AIMS Bioengineering*, 2(3):206–221, 2015.

[71] P. P. Slonimski. Adaptation respiratoire : développement du systéme hémoprotéique induit par l'oxygène. *Proc. 3rd int. Congr. Biochem.*, page 242, 1956.

[72] R. H. D. Deken. The crabtree effect: A regulatory system in yeast. *J. gen. Microbiol.*, 44:149–156, 1966.

[73] H. Li, Z. Ban, H. Qin, A. J. King, and G. Wang. A heteromeric membrane-bound prenyltransferase complex from hop catalyzes three sequential aromatic prenylations in the bitter acid pathway. *Plant Physiol.*, 167(3):650–659, 2015.

[74] G. Shen, D. Huhman, Z. Lei, J. Snyder, L. W. Sumner, and R. A. Dixon. Characterization of an isoflavonoid-specific prenyltransferase from *Lupinus albus*. *Plant. Physiol.*, 159(1):70–80, 2012. doi: 10.1104/pp.112.195271.

[75] F. Stehle, M. T. Stubbs, D. Strack, and C. Milkowski. Heterologous expression of a serine carboxipeptidase-like acyltransferase and characterization of the kinetic mechanism. *The FEBS Journal*, 275:775–787, 2008.

[76] R. D. Gietz and R. H. Schiestl. High-efficiency yeast transformation using the LiAc/SS carrier DNA/PEG method. *Nature Publishing Group*, 2(1):31–34, 2007.

[77] A. S. Karim, K. A. Curran, and H. S. Alper. Characterization of plasmid burden and copy number in *Saccharomyces cerevisiae* for optimization of metabolic engineering applications. *FEMS Yeast Res.*, 13(1):1–18, 2013.

[78] Shimadzu. Separation conditions: Fundamentals of a first-choice mobile phase, 2016. URL `http://www.shimadzu.com/an/lcms/support/lib/lctalk/60/60lab.html`.

[79] I. Sadowska-Bartosz, A. Paczka, M. Molon, and G. Bartosz. Dimethyl sulfoxide induces oxidative stress in the yeast *Saccharomyces cerevisiae*. *FEMS*, 13:820–830, 2013.

[80] C. Sousa, C. Nunes, M. Lúcio, H. Ferreira, J. Lima, J. Tavares, A. C. da Silva, and S. Reis. Effect of nonsteroidal anti-inflammatory drugs on the cellular membrane fluidity. *Journal of Pharmaceutical Sciences*, 97(8):3195–3206, 2007.

[81] K. Mukhopadhyay, A. Kohli, and R. Prasad. Drug susceptibilities of yeast cells are affected by membrane lipid composition. *Antimicrob. Agents Chemoter.*, 46(12):3695–3705, 2002.

Appendix A

Composition of yeast synthetic drop-out media without uracil and leucine

Table A.1: Amount of each component in one liter of the yeast synthetic drop-out media supplement without uracil and leucine

Component	Amount per liter of medium (mg)
Adenine hemisulfate	18
Alanine	76
Arginine hydrochloride	76
Asparagine monohydrate	76
Aspartic acid	76
Cysteine hydrochloride monohydrate	76
Glutamic acid monosodium salt	76
Glutamine	76
Glycine	76
Hystidine	76
myo-Inositol	76
Isoleucine	76
Lysine monohydrochloride	76
Methionine	76
p-Aminobenzoic acid potassium salt	8
Phenylalanine	76
Proline	76
Serine	76
Threonine	76
Tryptophan	76
Tyrosine disodium salt	76
Valine	76
	1546

Appendix B

Calculation of the growth parameters

The growth parameters calculated for describing the growth of *Sacharomyces cerevisiae* when exposed to different concentrations of olivetol were the lag time, the specific growth rate, and the doubling time.

The lag time can be seen by identifying the beginning of the exponential phase. By identifying that, one can take the duration of tha lag phase, that is the same as the lag time.

The specific growth rate is calculated only during the exponential phase. For that, the natural logarithm of the OD's of the exponential phase are expressed over the time and linearized. The slope of the regression line obtained is the specific growth rate. Furthermore, the doubling time is the quotient of the natural logarithm of two and the specific growth rate.